Author Manuscript

Author Manuscript

Author Manuscript

Author Manuscript

HHS Public Access

Author manuscript

Brain Struct Funct. Author manuscript; available in PMC 2018 July 01.

Published in final edited form as:

Brain Struct Funct. 2017 July ; 222(5): 2041–2058. doi:10.1007/s00429-016-1323-9.

Interhemispheric resting-state functional connectivity of the claustrum in the awake and anesthetized states

Jared B. Smith[a,b,e,1], **Zhifeng Liang**[b,c,d,2], **Glenn D.R. Watson**[b,d,e], **Kevin D. Alloway**[b,d,e,*], and **Nanyin Zhang**[b,c,d,*]

[a]Department of Engineering Science and Mechanics, Penn State University, University Park, PA, 16802 USA

[b]Center for Neural Engineering, Penn State University, University Park, PA, 16802 USA

[c]Department of Biomedical Engineering, Penn State University, University Park, PA,16802 USA

[d]The Huck Institutes of Life Sciences, Penn State University, University Park, PA, 16802 USA

[e]Department of Neural and Behavioral Sciences, Penn State University, Hershey, PA, 17033 USA

Abstract

The claustrum is a brain region whose function remains unknown, though many investigators suggest it plays a role in conscious attention. Resting-state functional magnetic resonance imaging (RS-fMRI) has revealed how anesthesia alters many functional connections in the brain, but the functional role of the claustrum with respect to the awake versus anesthetized states remains unknown. Therefore, we employed a combination of seed-based RS-fMRI and neuroanatomical tracing to reveal how the anatomical connections of the claustrum are related to its functional connectivity during quiet wakefulness and the isoflurane-induced anesthetic state. In awake rats, RS-fMRI indicates that the claustrum has interhemispheric functional connections with the mediodorsal thalamus (MD) and medial prefrontal cortex (mPFC), as well as other known connections with cortical areas that correspond to the connections revealed by neuroanatomical tracing. During deep isoflurane anesthesia, the functional connections of the claustrum with mPFC and MD were significantly attenuated, while those with the rest of cortex were not significantly altered. These changes in claustral functional connectivity were also observed when seeds were placed in mPFC or MD during RS-fMRI comparisons of the awake and deeply anesthetized states. Collectively, these data indicate that the claustrum has functional connections with mPFC and MD-thalamus that are significantly lessened by anesthesia.

Keywords

anatomical connectivity; anesthesia; claustrum; consciousness; functional connectivity

*Send correspondence to: Dr. Kevin Alloway, W-316 Millennium Science Complex, Penn State University, University Park, PA, 16802, USA, (814) 867-6413, kda1@psu.edu; Dr. Nanyin Zhang, W-341 Millennium Science Complex, Penn State University, University Park, PA, 16802, USA, (814) 867-4791, nxzbio@engr.psu.edu.

[1]Present Address: Molecular Neurobiology Laboratory, Salk Institute for Biological Studies, La Jolla, CA, 92037 USA

[2]Present Address: Laboratory of Comparative Neuroimaging, Institute of Neuroscience, Chinese Academy of Sciences, Shanghai 200031, China

The authors declare no competing financial interests.

Author Manuscript Author Manuscript Author Manuscript Author Manuscript

Introduction

The claustrum is a subcortical brain structure that is difficult to study due to its tortuous, elongated shape. Owing to this problematic geometry, classic lesion methodologies are nearly impossible, leaving investigators unable to assign a behavioral function to this enigmatic structure. As a result, the claustrum has remained an obscure brain structure that has only recently begun to gain attention (Goll et al. 2015).

In their landmark review, Crick and Koch proposed that the claustrum acts as the conductor of the cerebral orchestra by performing the integration necessary for conscious percepts (Crick and Koch 2005). In support of this hypothesis, anatomical tracing in rodents has shown that the claustrum is part of an interhemispheric circuit that interconnects modality-specific sensory and motor cortical areas, possibly to facilitate the corticocortical interactions needed for stable, global percepts (Smith and Alloway 2010, 2014; Smith et al. 2012b).

Beyond its proposed role in attention and perception, a recent clinical study suggests that electrical stimulation of the area around the claustrum, is sufficient to disrupt the conscious state (Koubeissi et al. 2014). However, other studies in human patients found no causal relationship between loss of consciousness and unilateral lesions of the claustrum (Duffau et al. 2007; Chau et al. 2015). No study, however, has identified the functional connections of the claustrum that are associated with the awake, conscious state. While non-invasive diffusion tensor imaging (DTI) has been used to investigate the static anatomical connections of the claustrum (Fernandez-Miranda et al. 2008; Park et al. 2012; Milardi et al. 2013; Arrigo et al. 2015), no study has characterized how the functional connectivity of this structure is dynamically altered with respect to conscious and unconscious states.

Resting-state functional magnetic resonance imaging (RS-fMRI) provides information about the functional connections of brain structures in different states based on the temporal synchronization of spontaneous fluctuations in blood-oxygenation-level dependent (BOLD) signals across voxels (Fox et al. 2005; Deco et al. 2011; Biswal 2012). The advantage of using fMRI for portraying claustral functional connectivity during the awake and anesthetized states is demonstrated by data showing that the conscious state is characterized by correlations in BOLD signals that are not constrained by direct anatomical connections (Barttfeld et al. 2015b). When compared to the unconscious state, the increased diversity of functional connectivity associated with the awake state can be mediated by multi-synaptic connections and an increase in network stochasticity that occurs with higher levels of spontaneous activity and cognitive-driven processing (Honey et al. 2009).

Here we demonstrate that the functional connectivity of the rat claustrum is altered between the awake and anesthetized states. Specifically, the claustrum has functional connections with the medial prefrontal cortex (mPFC) and mediodorsal (MD) thalamus that are significantly weakened in the isoflurane-induced, deeply anesthetized state. These interhemispheric connections between the claustrum, mPFC, and MD thalamus were further

Author Manuscript Author Manuscript Author Manuscript Author Manuscript

verified using neuroanatomical tracing. Together, these data identify novel functional networks involving the claustrum that are dynamically modified in the anesthetized state.

Materials and Methods

Resting state functional magnetic resonance imaging (RS-fMRI) experiments were performed on 42 adult male Long Evan rats (Charles Rivers) in previous studies (Liang et al. 2011, 2012, 2015). Anatomical tracing experiments were performed on 14 adult male Long Evans rats (Charles River). All procedures conformed to National Institute of Health standards and were approved by the Institutional Animal Care and Use Committee of Pennsylvania State University and the University of Massachusetts Medical School.

Resting State-fMRI

The RS-fMRI data acquired previously (Liang et al. 2011, 2012, 2015) were re-analyzed for the present study. The detailed methods for acquiring the data are fully described in the original reports. Briefly, 42 rats were acclimated to MRI restraint and noises for seven days. During the experimental setup, the rat was briefly anesthetized by isoflurane (2%) to secure the head and body in a restraining system with a built-in coil. Isoflurane was discontinued immediately after each rat was restrained, and sufficient time was given so that all rats were fully awake during imaging sessions (Shirey et al. 2015). Body temperature was maintained at 37 °C by a feedback controlled heating pad while the rats were imaged.

Among the 42 rats that were imaged in the awake state, 16 were imaged again during anesthesia induced by 1.5%–2% isoflurane administered via a nose cone. This concentration induces a deep anesthetic plane, characterized by loss of withdrawal reflexes, as well as a significant decrease in thalamic and cortical activity (Detsch et al. 1999; 2002; Shirey et al. 2015). Furthermore, 1.5–2% isoflurane produces an anesthetic state in which the electrocorticogram signal is dominated by a 1–2 Hz signal in the power spectrum, which is consistent with a loss of consciousness (Friedburg et al. 1999; Smith et al. 2012a; Alloway et al. 2014).

A Bruker 4.7T magnet with a dual ^{1}H radiofrequency head coil (Insight NeuroImaging Systems, Worcester, MA) was used for all MRI experiments. For each imaging session, rapid acquisition with relaxation enhancement (RARE) sequences were used to acquire anatomical images with the following parameters: TR = 2125 ms, TE = 50 ms, matrix size = 256 × 256, FOV = 3.2 × 3.2 cm^2, slice number = 18, slice thickness = 1 mm. Gradient-echo images were then acquired using the echo-planar imaging (EPI) sequence with the following parameters: TR = 1 s, TE = 30 ms, flip angle = 60°, matrix size = 64 × 64, FOV = 3.2 × 3.2 cm^2, slice number = 18, and slice thickness = 1 mm. Two hundred volumes were acquired for each scan, and six to nine scans were obtained for each session.

The RS-fMRI images of all rats were co-registered to a fully segmented rat atlas based on anatomical images by using Medical Image Visualization and Analysis Software (MIVA, http://ccni.wpi.edu/). Seed regions (see Figure 1) were identified from this segmented atlas and by comparing structural MRI images to the standard rat atlas (Paxinos and Watson, 2006). Preprocessing steps included motion correction with SPM8 (http://

Author Manuscript Author Manuscript Author Manuscript Author Manuscript

www.fil.ion.ucl.ac.uk/spm/), spatial smoothing (FWHM = 1 mm), regression of motion parameters and the signals of white matter and ventricles (to reduce their contributions of physiologic noise in the RS-fMRI signal), and 0.002–0.1 Hz band-pass filtering. Scans with excessive motion (>0.25 mm) were discarded.

Functional connectivity was evaluated using seed-based correlational analysis on a voxel-by-voxel basis (Liang et al. 2012). Seed time courses were obtained by averaging time courses from all voxels within individual seed regions. The Pearson cross-correlation coefficient between each seed time course and the time course of each individual voxel was then calculated. For partial correlation analysis, the correlational analysis was carried out in the same way, except that we controlled for (regressed out) the time courses of additional ROIs.

Correlation coefficients (i.e. *r* values) were transformed to z-scores using Fisher's z-transformation, and z-score maps were averaged across scans and animals to generate group maps. Analysis of variance across all pixels between awake and anesthetized states were performed to investigate an overall effect of anesthesia and t-tests were subsequently used to verify the significance of changes between the awake and anesthetized states for individual voxels.

Tracer injections

To confirm anatomical connectivity, rats were injected in the claustrum (8 attempts, 3 successful placements), prelimbic cortex (n=3), and MD-thalamus (n=3). To inject neuroanatomical tracers, rats were deeply anesthetized with an intramuscular injection of a mixture of ketamine (40 mg/kg) and xylazine (12 mg/kg). Animals then received injections of atropine methyl nitrate (0.5 mg/kg) to reduce bronchial secretions, dexamethasone (5 mg/kg) to minimize inflammation, and enroflaxin (2.5 mg/kg) to prevent infection. Next, animals were intubated per the oral cavity, fixed in a stereotaxic device (Kopf), and ventilated with oxygen and isoflurane (0.5–1.25%) to maintain a surgical plane of anesthesia plane throughout for the rest of the surgery and tracer injections.

Vital signs, including heart rate, blood oxygen, end-tidal carbon dioxide, and respiratory rate were continuously monitored (Surgivet). A rectal thermistor was inserted and attached to a homeothermic heating blanket to maintain body temperature at ~37.0°C. Eye ointment was applied to prevent corneal drying. A bolus of bupivacaine was injected subcutaneously before making an incision to expose the cranium. The skin was retracted, fascia was cleared, and a ground screw was placed in the skull behind lambda. Craniotomies were drilled to insert injection pipettes into the claustrum (1.5–2.5 mm rostral, 3.5–4.5 mm lateral), prelimbic cortex (2.5–3 mm rostral, 0.4–1.0 mm lateral), or MD-thalamus (1.5–2 mm caudal, 0.5–1 mm lateral). Location and extents of each brain region were based on the rat atlas and compared to subsequent analysis of Nissl stained alternate sections (Paxinos and Watson 2006).

For anterograde tracing experiments, Fluororuby (FR; D-1817, Invitrogen) or Biotinylated dextran amine (BDA; D-7135, Invitrogen) were injected. For retrograde tracing, Fluorogold (FG; H-22845, Fluoro-Chrome) was used. Deposits of FR were made by pressure injections, whereas BDA and FG were iontophoretically deposited through pulled glass pipettes (~30

Author Manuscript Author Manuscript Author Manuscript Author Manuscript

μm tips) using a 7s on/off duty cycle and applying the current through a silver wire (3 μA for FG, 5 μA for BDA, 10 μA for FR) for 30–45 minutes. Retention currents (−7.0 μA) were applied to the BDA and FG solutions while advancing the tracer-filled pipettes to their target depths (5–5.5 mm from pia for claustrum, 2–3 mm from pia for prelimbic cortex, 5–7 mm from pia surface for MD-thalamus), and the retention current was applied again when the pipettes were withdrawn from the injection site. After tracer injections, the incision was sutured, the wound was treated with antibiotic ointment, and the rats were returned to their home cage for 7–10 days to allow for tracer transport.

Histology

Animals were deeply sedated with intramuscular injections of ketamine (80 mg/kg) and xylazine (18 mg/kg) and perfused transcardially with heparinized saline, 4% paraformaldehyde, and 4% paraformaldehyde/10% sucrose. The brain was removed and stored in 4% paraformaldehyde/30% sucrose for 3–4 days until the brain sank.

Histological sections were acquired after the olfactory bulbs, cerebellum, and brainstem were removed. A slit was made into one hemisphere to denote the correct side while mounting. Each brain was sectioned on a freezing microtome, and the 60- μm sections were divided into three series. The first series was mounted and stained with thionin to reveal cytoarchitecture. The second series was processed for the presence of BDA as described previously (Smith et al. 2012a; Smith and Alloway 2014). Briefly, sections were rinsed in 0.3% H_2O_2 in phosphate buffered saline (PBS) to clear background enzymes, washed twice with 0.3% Triton-X-100 (TX-100) in 0.1M PBS, and then incubated for 2 hours in avidin-biotin horse radish peroxidase solution mixed in 0.3% TX-100. Sections were rinsed twice in 0.1M PBS before being incubated in 0.05% diaminobenzidine, 0.0005% H_2O_2, 0.05% $NiCl_2$, and 0.02% $CoCl_2$ in 0.1M tris buffer (pH = 7.2) for approximately 10 min to visualize the tracer. The reaction was stopped by two washes in 0.1M PBS. Sections were mounted, air dried, dehydrated in ethanol, defatted in xylene, and coverslipped with Cytoseal. The third series was processed for fluorescent labeling by simply mounting, dehydrating, defatting and coverslipping.

Anatomical analysis

Tracer labeling was analyzed with an Olympus BH-2 microscope equipped with a pair of X-Y optical transducers (MDPlot, Accustage). Both BDA and Nissl-stained sections were visualized in brightfield, whereas FR was visualized with a TRITC filter cube (41002; Chroma Technologies) and FG was visualized with a near UV filter cube (11000v2; Chroma Technologies). Digital reconstructions of the labeling patterns were created by plotting labeled cells and terminals relative to cytoarchitectural boundaries. A Retiga EXCCD digital camera mounted on the BH-2 microscope was used to take brightfield and fluorescent photomicrographs. Higher magnification images were acquired with a confocal microscope (Olympus Fluoview 1000), allowing us to show FR-labeled terminals (543 nm excitation, 565–630 nm detection) intermingled with FG-labeled neurons (405 nm excitation, 410–460 nm detection).

Author Manuscript Author Manuscript Author Manuscript Author Manuscript

Digital reconstructions of tracer labeling were analyzed using MDPlot software (version 5.1 Accustage). Consistent with the fact that Gng2 protein is localized in the claustrum at rostrocaudal coordinates that also contain the striatum, we plotted labeled cells and terminals in those sections where the striatum was present (Mathur et al. 2009). In addition to neuron and terminal counts, overlap analysis was performed by superimposing a grid of 50-μm^2 bins. Overlap bins were defined as containing a minimum of four FR-labeled terminals and one FG-labeled neuron. Total overlap was then expressed as a percentage of total number of labeled bins. Statistical analyses were performed with Origin software (version 8.0, Origin Lab).

Results

Functional connectivity of the claustrum in the awake and anesthetized states

To investigate the functional connectivity of the claustrum, we performed RS-fMRI on awake rats trained to remain quiescent while restrained during functional imaging (Liang et al. 2011, 2012, 2015). Seed-based correlational analysis was used on a voxel-by-voxel basis, and the locations of the claustral seeds are presented in structural MRIs in Figure 1. We characterized the whole-brain functional connectivity of the claustrum in both the awake and isoflurane-induced, deeply anesthetized states as shown in Figure 2. Seed regions were identified by comparing structural MRI images to the standard atlas (Paxinos and Watson, 2006) along with the MIVA atlas (described in Methods). For claustrum seeds, the voxels immediately ventral and lateral to the external capsule were used, at rostrocaudal levels containing the neostriatum as previously described (Mathur et al 2009).

In the awake state (Fig. 2a), the claustrum has strong functional connections with the cortex of both hemispheres, which confirms our previous studies showing that the claustrum is anatomically connected with the contralateral hemisphere (Smith and Alloway 2010, 2014; Smith et al. 2012b). In addition, the claustrum is functionally connected with the medial prefrontal cortex (mPFC), the surrounding cortical areas (i.e., cingulate and agranular motor cortices), and with more distant cortical areas (i.e., retrosplenial cortex). We also observed strong functional connections with the contralateral claustrum, even though no rodent studies have ever reported that the claustrum has direct anatomical connections with its counterpart in the contralateral hemisphere. Furthermore, RS-fMRI analysis in the awake state indicates that the claustrum has moderately-strong functional connections with the mediodorsal (MD) thalamus and widespread parts of sensory and association cortex.

Administration of isoflurane produced significant changes in the claustrum-based functional network compared to the awake state. Specifically, as shown by Figure 2, functional connections of the claustrum with mPFC and MD-thalamus were markedly decreased in the deeply anesthetized state. Furthermore, as indicated by Figure 3, claustrum connections with mPFC and MD-thalamus were significantly reduced based on a voxel by voxel statistical analysis of the differences in the claustrum seeded connectivity maps between the awake and the deeply anesthetized states (two-tailed t-tests, showing only significant t-values with $p<0.05$ based on False Discovery Rate). By contrast, the functional connections of the claustrum with the cingulate and agranular motor cortex, as well as with the contralateral claustrum, appeared unchanged (no significant differences) in the anesthetized state.

Author Manuscript Author Manuscript Author Manuscript Author Manuscript

Qualitatively similar results were obtained in both hemispheres regardless of whether the unilateral seed was placed in the left or right claustrum (data not shown). Collectively, these results indicate that the anesthesia-induced changes in claustrum connectivity are linked to specific brain regions.

To verify the specificity of our claustrum seed for revealing claustrum-related networks, we also placed seeds in the adjacent insular cortex, which is located just lateral to the claustrum. In the awake state, the unilateral insular cortex seed (Fig. 4a,b) showed strong functional connectivity with insular cortex in the contralateral hemisphere, but not with either mPFC or MD. In the deeply anesthetized state, the insular cortex seed revealed a functional connection with cingulate cortex, reminiscent of the “salience-like network” previously shown in anesthetized mice (Sforazzini et al. 2014b). The insular functional maps showed little resemblance to the claustrum-based network, and this indicates that the changes in the connectivity maps of the claustrum do not represent changes in blood flow to this nearby region.

An additional control experiment was performed using a seed based analysis of the striatum that lies medially adjacent to the claustrum (Fig. 4c,d). This analysis revealed bilateral, functional connections with mPFC, cingulate, and agranular motor cortex, as well as with MD thalamus, which were very similar to our claustrum seed analysis. However, our striatum seed analysis did not show strong connections with other widespread regions of sensory cortex that were observed in our claustrum seed analysis. The functional connections observed in our striatum seed match known inputs to this region of striatum, including bilateral inputs from cingulate cortex (Smith and Alloway 2014), agranular motor cortex (Alloway et al. 2009), and mPFC (Vertes 2004). In support of our claustrum seed analysis, each of these cortical regions also sends bilateral projections to claustrum in addition to their striatal projections. Furthermore, MD thalamus is known to project to both claustrum and striatum (Bay and Cadvar 2013). Finally, sensory cortical projections to striatum are known to terminate in more dorsolateral and caudal regions of striatum (Hoover et al. 2003; Hintiryan et al. 2016), explaining the lack of functional connections with sensory cortex from our striatal seed.

Our control seed analyses of adjacent insular cortex and striatum compared to the claustral seed thus show three different networks of functional connectivity. This suggests that our analyses are highly specific to the brain regions contained within a seed and represent their unique functional networks.

Anatomical connectivity of the claustrum

To determine how the functional connectivity of the claustrum relates to its anatomical connections, we compared the RS-fMRI data with the labeled connections revealed by conventional neuronal tracing. This aim was partly motivated by the fact that direct interhemispheric claustroclaustral connections were suggested by DTI data in humans (Milardi et al., 2015; Arrigo et al., 2015), but these findings have not been verified by neuronal tracing experiments in any species. To our knowledge, no study has injected the claustrum with an anterograde tracer in rats. Therefore, we injected the anterograde tracer, biotinylated dextran amine (BDA), into the claustrum of one hemisphere. Although some of

Author Manuscript Author Manuscript Author Manuscript Author Manuscript

the injected tracer diffused into the surrounding insular cortex, most of it occupied the claustrum (Fig. 2c,c′). These anterograde tracer deposits revealed a few labeled fibers in the contralateral insular cortex but not in contralateral claustrum (Fig. 2d′,e). Hence, the functional claustroclaustral connectivity observed in both awake and anesthetized rats cannot be mediated by direct, monosynaptic connections (Fig. 2a,b). Instead, the correlated BOLD signals in the claustrum of both hemispheres must be due to relatively strong multi-synaptic connections between the claustrum and the agranular cortex (Smith and Alloway 2010, 2014; Smith et al. 2012b).

Our tracing data revealed claustral projections to the MD-thalamus in both hemispheres, but the ipsilateral connections were much denser (Figure 2f). These bilateral anatomical connections provide a substrate for mediating the bilateral functional connections of the claustrum with the MD nuclei in the awake state. Despite these moderately-strong monosynaptic anatomical projections, functional connectivity between the claustrum and MD-thalamus was noticeably reduced in the anesthetized state. This finding demonstrates that monosynaptic anatomical connections between the claustrum and MD thalamus have functional connections in the awake state that are significantly lessened in the deeply anesthetized state.

In contrast to the bilateral projections to MD thalamus, most of the labeled projections from the claustrum terminated in ipsilateral cortical areas. This corroborates previous tracing studies conducted on multiple species (Crick and Koch 2005; Edelstein and Denaro 2004; Goll et al. 2015; Smith and Alloway 2010, 2014; Smith et al. 2012b; Mathur 2014; Smythies et al. 2014; Zingg et al. 2014; Wang et al. 2016). High resolution images of these claustrocortical projection terminals revealed thin fibers (Fig. 2j) across all layers of cortex with en passant boutons that resemble the classic drumstick appearance (Fig. 2j inset) that characterizes modulatory synapses (Crick and Koch 1998; Sherman and Guillery 1998). This type of presynaptic morphology was also observed in claustrocortical projections that contact dendritic spines of excitatory cells in cat visual cortex (da Costa et al. 2010).

Functional connectivity of mPFC in the awake and anesthetized states

As indicated by the structural MRIs in Figure 1, we also examined claustral connectivity after placing a unilateral seed in prelimbic cortex, which is a subdivision of rodent mPFC (Hoover and Vertes 2007). This part of mPFC was chosen because it showed the greatest change between the awake and anesthetized states in our claustrum-seed analysis (Figs. 2 and 3), and the specific seed region was assigned to voxels in our T1-weighted images that corresponded to PrL in the rodent atlas (Paxinos and Watson, 2006).

In the awake state, the mPFC has strong functional connections with the claustrum and MD nuclei in both hemispheres (Fig. 5a). Consistent with our claustrum seed analysis, isoflurane-induced, deep anesthesia caused significant changes in the functional network of the mPFC (Fig. 5b). Voxel by voxel statistical comparison of the connectivity maps generated by mPFC seeds in the awake and the anesthetized states are shown in Fig. 6. (two-tailed t-tests, showing only significant t-values with $p<0.05$ based on False Discovery Rate). During anesthesia, functional connectivity between mPFC and claustrum, and between mPFC and MD, were significantly attenuated (see pink arrows in Fig. 5a,b and in t-map in

Author Manuscript Author Manuscript Author Manuscript Author Manuscript

Fig. 6). These data are consistent with the results obtained when the seed was placed in the claustrum.

Anatomical connectivity of the mPFC

In parallel with the RS-fMRI analysis of mPFC, we characterized the anatomical projections of mPFC by injecting this region with an anterograde tracer in one hemisphere and a retrograde tracer in the other hemisphere of the same animal (Fig. 5c,d,e). This revealed an interhemispheric cortico-thalamo-cortical circuit (Fig. 5f,g) that involved the MD nucleus as well as other thalamic nuclei as described previously (Alloway et al. 2008; Negyessy et al. 1998; Smith and Alloway 2014).

These separate deposits of anterograde and retrograde tracers in mPFC of opposite hemispheres revealed a strong interhemispheric circuit that involved the claustrum (Fig. 5h,i,j). While most anterogradely-labeled projections from mPFC terminate in the contralateral claustrum, the retrogradely-labeled claustral neurons were located almost exclusively in the ipsilateral hemisphere. To quantify this relationship, we plotted the labeled neurons and terminals (Fig. 5i) throughout the rostro-caudal extent of the claustrum as delineated previously by the Gng2 protein (Mathur et al. 2009). Hemispheric differences in tracer labeling were significant (Fig. 7a,c; anterograde labeling: $F=26.0$, $p<0.00001$; retrograde labeling: $F=59.8$, $p<10^{-10}$), and confirmed that mPFC projects more to the contralateral than to the ipsilateral claustrum (paired t, $t=9.54$, $p<10^{-11}$), whereas the claustrum projects exclusively to ipsilateral mPFC (paired $t=8.07$, $p<10^{-9}$). Consequently, there was significantly more terminal-neuronal overlap in the claustrum of the hemisphere that received the retrograde tracer injection (Fig. 7b; $t=14.75$, $p<0.01$).

The interhemispheric functional connectivity of the claustrum was also confirmed by partial correlation analysis (Fig. 8). By removing correlations involving frontal cortex (including AGm, Cg, and PrL) in a unilateral claustrum-based seed analysis, the claustroclaustral correlations were noticeably attenuated (see pink arrows in Fig. 8). This manipulation suggests that the claustroclaustral functional connectivity observed in both the awake and anesthetized states is mediated by strong disynaptic connections through regions of frontal cortex that are not affected by anesthesia (mainly AGm and Cg).

Functional connectivity of MD thalamus in the awake and anesthetized states

Placement of a unilateral seed in nucleus MD (see Fig. 1) revealed strong bilateral functional connections with both the claustrum and mPFC when rats were awake (Fig. 9a). During isoflurane-induced, deep anesthesia, however, the functional connections of the MD nucleus with both the claustrum and mPFC were markedly reduced (Fig. 9b). These data corroborate the diminished functional connections observed in our claustrum- and mPFC-seed analyses. As observed with our claustrum seed analysis, isoflurane anesthesia caused significant changes in the functional network of MD thalamus. Voxel by voxel statistical comparison of our MD seed analysis between the awake and the anesthetized states are shown in Fig. 10 (two-tailed t-tests, showing only significant t-values with $p<0.05$ based on False Discovery Rate). During anesthesia, functional connectivity between MD thalamus and claustrum, as well as mPFC, was significantly attenuated (see pink arrows in Fig. 9a,b and Fig. 10). These

Author Manuscript Author Manuscript Author Manuscript Author Manuscript

results confirm anesthesia induced functional connectivity changes observed using claustrum and mPFC seed based analyses.

Anatomical connectivity of MD thalamus

We also made large tracer injections in nucleus MD (Fig. 9c) to verify its anatomical connectivity with the mPFC (Fig. 9d) and claustrum (Fig. 9e,f,g). Dense terminal and somal labeling was observed in the ipsilateral mPFC, including both PrL (Fig. 9d) and Cg (Fig. 9e), which matches the functional connectivity revealed by the MD seed in the awake state. Similarly, both anterograde and retrograde labeling were observed in the claustrum following tracer injections into MD, thereby indicating reciprocal connectivity, which has been previously observed in both rodents (Bay and Cadvar 2013; Mitchell 2015) and primates (Erickson et al. 2004). The anterogradely-labeled thalamoclaustral fibers were thin with drumstick shaped, terminals indicative of modulator type synapses (Crick and Koch 1998; Sherman and Guillery 1998), also observed for the claustrocortical projections (Fig. 2j).

Discussion

The anatomical connectivity of the claustrum is illustrated by a circuit diagram in Figure 11. Line widths depict connection strengths based on our neuronal tracing data. Together, neuronal tracing and resting-state functional connectivity demonstrate that the claustrum is involved in the bilateral coordination of many cortical areas. Furthermore, despite lacking a direct anatomical connection, the claustrum is functionally connected to the claustrum in the opposite hemisphere, likely via interhemispheric circuits involving mPFC, cingulate, and agranular motor cortex. Our seed-based RS-fMRI analysis indicates that the claustrum has previously unknown bilateral functional connections with MD-thalamus and mPFC in the awake state, which were verified by anatomical tracing. These claustral functional connections with mPFC and MD thalamus were significantly weakened in the isoflurane-induced, deeply anesthetized state. Finally, claustro-cortical and thalamo-claustral axonal terminals are thin and have modulator-type synaptic morphology.

Physiological functions of the claustrum

Many investigators have hypothesized that the claustrum is responsible for binding multisensory information (Crick and Koch 2005; Smythies et al. 2012), coordinating brain regions that mediate attention mechanisms (Smith and Alloway 2014; Goll et al. 2015), or for detecting salient stimuli (Mathur 2014), but no study has conducted conclusive tests for these hypotheses. Most claustral studies have characterized the cytoarchitecture, neurochemical make-up, and anatomical connectivity of the claustrum (for review Edelstein and Denaro 2004; Mathur 2014; Smythies et al. 2014), but very few have characterized its physiological properties. Stimulation studies in cats have shown that the claustrum exerts a mix of excitatory and inhibitory effects on cortex (reviewed in Sherk 2014) and neuronal recordings in the claustrum have revealed modality-specific responses to sensory stimulation (LeVay and Sherk 1981; Olson and Graybiel 1980; Remedios et al. 2010, but see Spector et al. 1974 for multisensory responsive claustral neurons in cat), an increase in firing rate

Author Manuscript Author Manuscript Author Manuscript Author Manuscript

during motor movements (Shima et al. 1991), as well as higher-order encoding of “objects” or “place” (Jankowski and O’Mara 2015).

Though we did not perform electrophysiological recordings in the claustrum, our anatomical data suggest that claustro-cortical and thalamo-claustral transmission are mediated by modulator type synapses. This conclusion is drawn from the anatomical observation of small, “drum-stick”-like branched terminals extending from claustral projection fibers, similar to the structure of corticothalamic fibers known as “modulator-type” terminals (Sherman and Guillery 1998). This bouton morphology is associated with slow propagation (due to thin axon diameter) and small amplitude post-synaptic potentials that exhibit paired-pulse facilitation, which suggests that these connections modify activity in their target structures instead of transmitting high fidelity information with a strong, driving force (Crick and Koch 1998; da Costa et al. 2010; Sherman and Guillery 1998). Our anatomical results beckon future electrophysiological studies to characterize the influence of claustral synapses on its targets, and suggests that the claustrum plays a role in modulating cortical activity, perhaps to alter cortical oscillations (Smythies et al. 2012).

Our study is the first to assess the whole-brain, functional network connectivity of the claustrum during the awake and anesthetized states. Our results reveal claustral involvement in vast interhemispheric functional networks, in support of previous anatomical tracing studies (Smith and Alloway 2010, 2014; Smith et al 2012b). Interestingly, we identify a functional connection between the claustra of each hemisphere that seems to be mediated by interhemispheric connections through the corpus callosum with mPFC, cingulate, and motor cortex. Furthermore, functional connectivity studies done in acallosal mice show a loss of interhemispheric functional connectivity between motor cortex and the region of the claustrum (see Fig. 3 in Sforazzini et al 2014a). Together these data suggest a highly synchronized, interhemispheric circuit involving regions of frontal cortex and the claustrum, whose function as yet remains unknown.

Insight into the function of these interhemispheric claustral circuits may emerge from comparative studies across species. Bilateral corticoclaustral projections to the claustrum in primates are known (Künzle 1975). However, in contradiction to the results in our current study in rodents, a recent anatomical tracing study from mPFC in marmosets observed that projections to the ipsilateral claustrum were much stronger than those in the contralateral claustrum (Reser et al. 2016). Claustral connectivity with cortex varies across species, including across different primate lineages (Sherk 1986). Our discovery of bilateral corticoclaustral connections in the rat prompted the view that the claustrum has a role in coordinating cortical areas that process sensorimotor information relevant to bilaterally-coordinated movements such as eye movements or exploratory whisking (Alloway et al. 2009; Smith et al. 2010; 2014). Analysis of the interhemispheric cortico-claustral projections from supplementary or frontal eye fields in primates would allow direct inter-species comparison of cortico-subcortical networks controlling homologous behaviors (with the caveat that eye movements in rodents and primates are qualitatively different). With regard to interhemispheric functional circuitry, differences in the weighting of interhemispheric projections of mPFC between rodent and marmoset provides an opportunity for exploring

Author Manuscript Author Manuscript Author Manuscript Author Manuscript

the relationship between anatomical and functional networks, but requires future RS-fMRI experiments in marmosets.

Based on recent clinical evidence, the claustrum has been hypothesized to play a role in the networks underlying the conscious state (Koubeissi et al. 2014; but see Duffau et al. 2007 and Chau et al. 2015 for an opposing view). Our data show that the claustrum is functionally connected with mPFC and MD thalamus in the awake state, and these functional connections are significantly reduced during deep anesthesia even though other functional connections persist. These data pinpoint which claustral connections are functionally affected by isoflurane anesthesia, but allow only limited speculation on functional mechanisms. One limitation is that we only investigated the awake and deeply anesthetized state, and not the transition period between these states, which may provide insight into the functional mechanism by which consciousness is lost during anesthesia.

To ascertain the specificity of our seed based analysis to a region as small as the claustrum, we performed control seed-based analysis of regions directly medial (striatum) and lateral (insular cortex) to the claustrum. We found that both claustrum and striatum have strong functional connections with AGm, Cg and PrL cortex, which is consistent with known anatomical data demonstrating that these cortical regions project to both the striatum and claustrum (Alloway et al. 2009, Smith and Alloway 2014, Vertes 2004). This anatomical data is further supported by our mPFC seed analysis in the awake state, which shows strong connections to both claustrum and striatum (see Figure 5a).

Functional connectivity was observed between MD thalamus with both the claustrum and striatum, matching the anatomical connections revealed by our anterograde tracing experiments on the MD thalamus (see Figure 9e, f). However, our striatum seed analysis did not show strong connections with other widespread regions of sensory cortex, which were observed in our claustrum seed analysis, owing to striatal topography whereby sensory projections terminate in more dorsolateral and caudal regions (Hoover et al. 2003; Hintiryan et al. 2016).

Seeds placed in the insular cortex, which lies directly adjacent to the claustrum revealed a functional network that differed substantially from the claustral functional network. This insular seed also confirmed the presence of a network resembling the human “salience network” (Seeley 2007), which was also observed in RS-fMRI experiments on isoflurane anesthetized mice (Sforazzini et al. 2014b). Surprisingly, our “salience-like network” was more pronounced in the anesthetized state, with strong functional connections between insula and cingulate cortex, compared to the weaker insulo-cingular connections we observed in the awake state. The reasons behind this difference are unclear, but warrant further investigation into this network’s sensitivity to anesthesia.

The main hypotheses concerning the function of the claustrum have focused on neural mechanisms that mediate multisensory integration, salience detection, and attention. Though we did not test the effects of sensory stimulation, our data show functional connectivity between the claustrum and widespread regions of sensory cortex in both hemispheres. This confirms anatomical studies showing that the claustrum is connected with all sensory areas,

Author Manuscript Author Manuscript Author Manuscript Author Manuscript

and provides evidence that the claustrum is involved in multisensory processing. However whether these modalities are integrated at a single cell level within the claustrum remains contradictory (Spector et al. 1974; Remedios et al. 2010).

With respect to salience detection, in our insula cortex seed analysis we observed strong functional connections with cingulate cortex, reminiscent of the rodent “salience-like” network (Seeley 2007; Sforazzini et al. 2014b; Gozzi and Schwarz 2016). Interestingly, our claustrum seed analysis also showed strong functional connectivity with cingulate cortex, suggesting the claustrum is involved with the “salience-like” network and providing indirect evidence for a role of the claustrum in salience-detection.

Our data do not directly address the role of the claustrum in attention, but we detected strong functional connectivity between the claustrum and frontal cortical regions (Cg, AGm) that are believed to play a role in directed attention as part of their role in motor control (Reep and Corwin 2009; Smith and Alloway 2010; 2014). Interestingly, we found the strongest functional connectivity of the claustrum with cortex was to these attention-related regions of frontal cortex, whereas weaker connections were observed with sensory cortex. This further emphasizes the potential role of the claustrum in mechanisms of attention. When considered with our anatomical data that claustrocortical projections are modulator type synapses (thought to feature paired-pulse facilitation), our data suggest that the claustrum may modulate attention through frontal cortex (AGm, Cg, PrL). However, further studies are needed to directly test this hypothesis.

Effects of general anesthesia on functional connectivity underlying loss of consciousness

The use of anesthetics to study mechanisms of consciousness require understanding both the pharmacological effects of the drug on brain physiology, as well as the systems-level circuit changes that lead to a loss of consciousness. In our experiments relatively high doses (1.5%–2%) of isoflurane were administered to assure loss of consciousness while the rat was in the magnet. As a result, the changes in functional connectivity observed here may differ from what would have been observed if lower or higher doses had been administered. Anesthesia is thought to have a dose dependent effect on functional connectivity (Peltier et al. 2005; Vincent et al. 2007; Deshpande et al. 2010; Boveroux et al. 2010; Liu et al. 2011; Nasrallah et al. 2014; Barttfeld et al. 2015a). Moderate to high doses cause significant changes in functional connectivity compared to the awake state, whereas functional connectivity under lower doses of anesthesia have in some cases been shown to be similar to the awake state (Barttfeld et al. 2015b; Taqliazucchi et al. 2016; Gozzi and Schwarz 2016).

In general, loss of consciousness under many anesthetics is thought to result from a disruption at the level of the thalamus (Alkire 2008; Alkire and Miller 2005; Alkire et al. 2008; Hudetz 2012; Hwang et al. 2012; Mashour 2006; Mhuircheartaigh et al. 2010). Isoflurane hyperpolarizes thalamo-cortical neurons (Langmoen et al. 1995; Ries and Puil 1999a,b), and this may also apply to thalamo-claustral neurons, thereby reducing the functional connectivity of MD thalamus with claustrum as we report here. Isoflurane diminishes excitation by reducing glutamate release and increases inhibition via GABAergic mechanisms, thereby substantially altering neural activity in a dose dependent manner (Joksovic and Todorovic 2010; Langmoen et al. 1995; Liachenko et al. 1999; Wakamori et

Author Manuscript Author Manuscript Author Manuscript Author Manuscript

al. 1991; Ying et al. 2009). This suggests that lower or intermediate levels of isoflurane-induced sedation may have different changes in functional connectivity compared to the deep levels of anesthesia used here.

The literature on the relationship between anesthesia and functional connectivity of thalamus is expansive and at times conflicting (for comprehensive reviews see Hudetz 2012; Gozzi and Schwarz, 2016). Consistent with our current findings, many studies analyzing whole brain changes in functional connectivity between awake and anesthetized states find robust degradation of thalamocortical networks (Akeju et al. 2014; Boveroux et al. 2010; Taqliazucchi et al. 2016; Nasrallah et al. 2014; Schroter et al. 2012). In support of these findings, other studies performed only in the anesthetized state found no functional connectivity with thalamus (Vincent et al. 2007; Hutchison et al. 2011). In contrast, some studies did observe functional thalamocortical connectivity in the anesthetized state (Schwarz et al. 2013; Grandjean et al. 2014; Sforazzini et al. 2014b), sometimes even at relatively high doses (Liu et al. 2011; 2013).

Differences in thalamocortical responsivity to anesthesia seem to reflect variations in anesthetic sensitivity for different thalamic nuclei, causing some thalamocortical connections under anesthesia to be lost and others to be maintained. As an example, primary somatosensory nuclei in the thalamus are known to continue to respond to sensory stimuli even under deep sedation, whereas higher order sensory thalamic nuclei lose their responses (Diamond et al. 1992). With regards to RS-fMRI functional connectivity, we have previously shown a more severe degradation of thalamocortical functional connectivity of cognitive circuits from a seed placed in infralimbic cortex between the awake and anesthetized states compared to primary somatosensory cortex thalamocortical connections (Liang et al. 2015). Indeed, other studies looking purely at primary sensory networks do not report thalamocortical functional degradation at even high doses of anesthesia (Liu et al. 2011; 2013). In support of this finding, other studies have found that thalamocortical functional connectivity in “low-level sensory” networks was preserved during anesthesia compared to the awake state, whereas thalamocortical functional connections in other networks, particularly frontal networks (including DMN) were significantly decreased (Boveroux et al. 2010; Akeju et al. 2014; Taqliazucchi et al. 2016). These results seem to confirm that different thalamocortical circuits show varying sensitivity to anesthesia, particularly in terms of functional connectivity.

In the analyses reported in this paper, we saw similar results. Wherein claustrum connectivity with mPFC and MD thalamus was degraded under anesthesia, bilateral connections with sensorimotor cortex persisted. This result may relate to the increased sensitivity of higher-order circuits to anesthetics, and may provide important clues to the emergence of the awake, conscious state out of these higher-order networks.

The reasons for these dramatic differences in thalamocortical functional connectivity patterns observed under different anesthetic regimes or across different thalamocortical circuits remains unresolved, but warrants caution when interpreting functional connectivity data. These disparities may be due to the particular anesthetic regimen employed, inter-species differences, dissimilarities in physiologic state of the subjects (i.e. temperature,

Author Manuscript Author Manuscript Author Manuscript Author Manuscript

oxygenation, etc.), variations in data processing, or other methodological variations (for discussions of these topics see Grandjean et al. 2014; Gozzi and Schwarz 2016). Whether the claustrum circuit dynamics described here occur under different anesthetics and other species requires future studies.

Relationship of the claustrum to the rodent default mode network and cognition

The mPFC is part of the rodent default mode network, which is thought to be active when the brain is idle, in the absence of other mental functions such as sensory perception and motor planning (Fox et al. 2005; Lu et al. 2012; Mitchell 2015; Gozzi and Schwarz 2016). By using a seed based analysis approach, our data suggest that the claustrum and MD thalamus are anatomically and functionally connected to mPFC, and thus may be involved in the rodent default mode network. Previous studies in both humans (He et al. 2015) and rodents (Sforazzini et al 2014b; Schwarz et al 2013) using seed-based approaches have indicated that thalamus is functionally connected to the default mode network (reviewed in Gozzi and Schwarz 2016). Our data expand on these studies to indicate that the claustrum is also functionally connected to the mPFC, and thus likely to influence the default mode network.

This finding provides indirect evidence for a role of the claustrum in supporting the awake state. Previous studies have suggested that the default mode network displays a decrease in functional connectivity during anesthesia induced loss of consciousness (Vincent et al. 2007; Liu et al. 2011; Akeju et al. 2014; Boveroux et al. 2010; but see Sforazzini et al. 2014b; Schwarz et al 2013 for cases in rodents where DMN functional connectivity was preserved in the anesthetized state and Greicius et al. 2008 in humans) and patients with disorders of consciousness, such as coma and vegetative states (Vanhaudenhuyse et al. 2010). Thus, future studies investigating the relationship of the default mode network and loss of consciousness may reveal degradations in functional connectivity between mPFC and MD thalamus with the claustrum.

Beyond the default mode network, the mPFC and MD circuits are believed to be involved in multiple cognitive processes (reviewed in Mitchell 2015). Our data demonstrate that these brain regions have interhemispheric anatomical and functional connections with the claustrum. Together, these findings suggest that the claustrum may play a role in mediating the interhemispheric coordination of cognitive related information.

Technical limitations of RS-fMRI to assess structural connectivity in the anesthetized state

The data in our study shed light on the mechanisms underlying RS-fMRI and the limitations of its interpretability. A previous study using RS-fMRI in awake humans and primates suggests that functional networks resemble the underlying anatomical network structure, as determined by DTI (Greicius et al. 2009). In contrast, another recent study emphasizes that the awake state demonstrates functional connections that exist beyond the constraints of the structural (anatomical) connectivity (Barttfeld et al. 2015b). By comparing our RS-fMRI data to our anatomical tracing results, we showed that functional connectivity in the awake and anesthetized state can both differ from the underlying anatomical substrate. While the claustrum has strong anatomical connections with MD-thalamus, we found that this

Author Manuscript Author Manuscript Author Manuscript Author Manuscript

connection was most obviously detected by RS-fMRI only when the animal was awake. Furthermore, even though the anatomical data indicate that the claustrum is not monosynaptically connected with its counterpart in the opposite hemisphere, RS-fMRI revealed functional claustroclaustral connectivity in both the awake and anesthetized states, probably because of the strong interhemispheric anatomical connections between the claustrum and agranular motor cortex (Smith and Alloway 2010, 2014; Smith et al. 2012b). Hence, our results suggest a tenuous relationship between anatomical and functional connectivity, and this emphasizes the need for caution in interpreting RS-fMRI data, particularly when inferring structural connectivity from functional connectivity, even in the anesthetized state.

A final complication of using isoflurane in our experiments is its vasoactive effects, which may alter the blood oxygen level dependent (BOLD) signal measured with fMRI. Isoflurane is a potent vasodilator and it decreases brain temperature (Masamoto and Kanno 2012; Shirey et al. 2015). These effects occur throughout the entire brain and therefore should affect all functional connections to the same extent, minimizing their impact on our results. Furthermore, though neurovascular coupling has been shown to be altered by isoflurane, the relationship between increases in neural activity and increases in BOLD persist, which suggests that the BOLD measurements in our study reflect underlying changes in neural activity (Franceschini et al. 2010; Masamoto and Kanno 2012).

Acknowledgments

This work was supported by NIH grants R01NS085200 and R01MH098003 awarded to N. Zhang, and NIH grant R01NS37532 awarded to K.D. Alloway. J.B.S., N.Z. and K.D.A. designed research; J.B.S. and G.D.R.W. performed neuroanatomical tracing experiments and J.B.S. analyzed the data, Z.L. and N.Z. performed and analyzed all resting state fMRI experiments. J.B.S., Z.L., and K.D.A. wrote the manuscript. All authors revised and approved the manuscript.

References

Akeju O, Loggia ML, Catana C, Pavone KJ, Vazquez R, Rhee J, Ramirez VC, Chonde DB, Izquierdo-Garcia D, Arabasz G, Hsu S, Habeeb K, Hooker JM, Napadow V, Brown E, Purdon PL. Disruption of thalamic functional connectivity is a neural correlate of dexmedetomidine-induced unconsciousness. eLife. 2014; 3:e04499.doi: 10.7554/eLife.04499 [PubMed: 25432022]

Alloway KD, Olson ML, Smith JB. Contralateral corticothalamic projections from MI whisker cortex: potential route for modulating hemispheric interactions. J Comp Neurol. 2008; 510:100–116. DOI: 10.1002/cne.21782 [PubMed: 18615539]

Alloway KD, Smith JB, Beauchemin KJ, Olson ML. Bilateral projections from rat MI whisker cortex to the neostriatum, thalamus, and claustrum: forebrain circuits for modulating whisking behavior. J Comp Neurol. 2009; 515(5):548–564. DOI: 10.1002/cne.22073 [PubMed: 19479997]

Alloway KD, Smith JB, Watson GDR. Thalamostriatal projections from the medial posterior and parafasicular nuclei have distinct topographic and physiologic properties. J Neurophysiol. 2014; 111:36–50. DOI: 10.1152/jn.00399.2013 [PubMed: 24108793]

Alkire MT. Loss of effective connectivity during general anesthesia. Int Anesthesiol Clin. 2008; 46(3): 55–73. DOI: 10.1097/AIA.0b013e3181755dc6

Alkire MT, Miller J. General anesthesia and the neural correlates of consciousness. Prog Brain Res. 2005; 150:229–244. DOI: 10.1016/S0079-6123(05)50017-7 [PubMed: 16186027]

Alkire MT, Hudetz AG, Tononi G. Consciousness and anesthesia. Science. 2008; 322(5903):876–880. DOI: 10.1126/science.1149213 [PubMed: 18988836]

Author Manuscript Author Manuscript Author Manuscript Author Manuscript

Arrigo A, Mormina E, Calamuneri A, Gaeta M, Granata F, Marino S, Anastasi GP, Milardi D, Quartarone A. Inter-hemispheric claustral connections in human brain: a constrained spherical deconvolution-based study. Clin Neuroradiol. 2015; in press. doi: 10.1007/s00062-015-0492-x

Barttfeld P, Bekinschtein TA, Salles A, Stamatakis EA, Adapa R, Menon DK, Sigman M. Factoring the brain signatures of anesthesia concentraion and level of arousal across individuals. Neuroimage Clin. 2015a; 9:385–391. DOI: 10.1016/j.nicl.2015.08.013 [PubMed: 26509121]

Barttfeld P, Uhriq L, Sitt JD, Sigman M, Jarraya B, Dehaene S. Signature of consciousness in the dynamics of resting-state brain activity. Proc Natl Acad Sci USA. 2015b; 112(3):887–892. DOI: 10.1073/pnas.1418031112 [PubMed: 25561541]

Bay HH, Cadvar SS. Regional connections of the mediodorsal thalamic nucleus in the rat. J Integr Neurosci. 2013; 12(2):201–219. DOI: 10.1142/S021963521350012X [PubMed: 23869861]

Biswal BB. Resting state fMRI: A personal history. Neuroimage. 2012; 62:938–944. DOI: 10.1016/j.neuroimage.2012.01.090 [PubMed: 22326802]

Boveroux MD, Vanhaudenhuyse A, Bruno M-A, Noirhomme Q, Lauwick S, Luxen A, Degueldre C, Plenevaux A, Schnakers C, Phillips C, Brichant J-F, Bonhomme V, Maquet P, Greicius MD, Laureys S, Boly M. Breakdown of within- and between network resting state functional magnetic resonance imaging connectivity during propofol-induced loss of consciousness. Anesthesiology. 2010; 113:1038–1053. DOI: 10.1097/ALN.0b013e3181f697f5 [PubMed: 20885292]

Chau A, Salazar AM, Krueger F, Cristofori I, Grafman J. The effect of claustrum lesions on human consciousness and recovery of function. Conscious Cogn. 2015; 36:256–264. DOI: 10.1016/j.concog.2015.06.017 [PubMed: 26186439]

Crick F, Koch C. Constraints on cortical and thalamic projections: the no-strong-loops hypothesis. Nature. 1998; 391(6664):245–250. DOI: 10.1038/34584 [PubMed: 9440687]

Crick FC, Koch C. What is the function of the claustrum? Philos Trans R Soc Lond B Biol Sci. 2005; 360(1458):1271–1279. DOI: 10.1098/rstb.2005.1661 [PubMed: 16147522]

da Costa NM, Fursinger D, Martin KAC. The synaptic organization of the claustral projection to the cat's visual cortex. J Neurosci. 2010; 30(39):13166–13170. DOI: 10.1523/JNEUROSCI.3122-10.2010 [PubMed: 20881135]

Deco G, Jirsa VK, McIntosh AR. Emerging concepts for the dynamical organization of resting-state activity in the brain. Nat Rev Neuro. 2011; 12:43–56. DOI: 10.1038/nrn2961

Deshpande G, Kerssens C, Sebel PS, Hu X. Altered local coherence in the default mode network due to sevoflurane anesthesia. Brain Res. 2010; 1318:110–121. DOI: 10.1016/j.brainres.2009.12.075 [PubMed: 20059988]

Detsch O, Kochs E, Siemers M, Bromm B, Vahle-Hinz C. Differential effects of isoflurane on excitatory and inhibitory synaptic inputs to thalamic neurons in vivo. Br J Anaesth. 2002; 89(2):294–300. [PubMed: 12378670]

Detsch O, Vahle-Hinz C, Kochs E, Siemers M, Bromm B. Isoflurane induces dose-dependent changes of thalamic somatosensory information transfer. Brain Res. 1999; 829(1–2):77–89. [PubMed: 10350532]

Diamond ME, Armstrong-James M, Budway MJ, Ebner FF. Somatic sensory responses in the rostral sector of the posterior group (POm) and in the ventral posterior medial nucleus (VPM) of the rat thalamus: dependence on the barrel field cortex. J Comp Neurol. 1992; 319:66–84. DOI: 10.1002/cne.903190108 [PubMed: 1592906]

Duffau H, Mandonnet E, Gatignol P, Capelle L. Functional compensation of the claustrum: lessons from low-grade glioma surgery. J Neurooncol. 2007; 81:327–329. DOI: 10.1007/s11060-006-9236-8 [PubMed: 16944310]

Edelstein LR, Denaro FJ. The claustrum: a historical review of its anatomy, physiology, cytochemistry and functional significance. Cell and Molec Biol (Noisy-le-grand). 2004; 50(6):675–702. [PubMed: 15643691]

Erickson SL, Melchitzky DS, Lewis DA. Subcortical afferents of the lateral mediodorsal thalamus in cynomolgus monkeys. Neuroscience. 2004; 129(3):675–690. DOI: 10.1016/j.neuroscience.2004.08.016 [PubMed: 15541889]

Author Manuscript Author Manuscript Author Manuscript Author Manuscript

Fernandez-Miranda JC, Rhoton AL Jr, Kakizawa Y, Choi C, Alvarex-Linera J. The claustrum and its projection system in the human brain: a microsurgical and tractographic anatomical study. J Neurosurg. 2008; 108(4):764–774. DOI: 10.3171/JNS/2008/108/4/0764 [PubMed: 18377257]

Fox MD, Snyder AZ, Vincent JL, Corbetta M, Van Essen DC, Raichle ME. The human brain is intrinsically organized into dynamic, anticorrelated functional networks. Proc Natl Acad Sci USA. 2005; 102(27):9673–9678. DOI: 10.1073/pnas.0504136102 [PubMed: 15976020]

Franceschini MA, Radhakrishnan H, Thakur K, Wu W, Ruvinskaya S, Carp S, Boas DA. The effect of different anesthetics on neurovascular coupling. Neuroimage. 2010; 51:1367–1377. DOI: 10.1016/j.neuroimage.2010.03.060 [PubMed: 20350606]

Friedberg MH, Lee SM, Ebner FF. Modulation of receptive field properties of thalamic somatosensory neurons by the depth of anesthesia. J Neurophysiol. 1999; 81(5):2243–52. [PubMed: 10322063]

Goll Y, Atlan G, Citri A. Attention: the claustrum. Trends Neurosci. 2015; 38(8):486–495. DOI: 10.1016/j.tins.2015.05.006 [PubMed: 26116988]

Gozzi A, Schwarz AJ. Large-scale functional connectivity networks in the rodent brain. Neuroimage. 2016; 127:496–509. DOI: 10.1016/j.neuroimage.2015 [PubMed: 26706448]

Grandjean J, Schroeter A, Batata I, Rudin M. Optimization of anesthesia protocol for resting-state fMRI in mice based on differential effects of anesthetics on functional connectivity patterns. Neuroimage. 2014; 102(2):838–847. DOI: 10.1016/j.neuroimage.2014.08.043 [PubMed: 25175535]

Greicius MD, Kiviniemi V, Tervonen O, Vainionpää V, Reiss AL, Menon V. Persistent default- mode network connectivity during light sedation. Human Brain Mapping. 2008; 29(7):839–847. DOI: 10.1002/hbm.20537.Persistent [PubMed: 18219620]

Greicius MD, Supekar K, Menon V, Dougherty F. Resting-state functional connectivity reflects structural connectivity in the default mode network. Cereb Cortex. 2009; 19:72–78. DOI: 10.1093/cercor/bhn059 [PubMed: 18403396]

He JH, Cui Y, Song M, Yang Y, Dang YY, Jiang TZ, Xu RX. Decreased functional connectivity between the mediodorsal thalamus and default mode network in patients with disorders of consciousness. Acta Neurol Scand. 2015; 131(3):145–151. DOI: 10.1111/ane.12299 [PubMed: 25263131]

Hintiryan H, Foster NN, Bowman I, Bay M, Song MY, Gou L, Yamashita S, Bienkowski MS, Zingg B, Zhu M, Yang XW, Shih JC, Toga AW, Dong H-W. The mouse cortico-striatal projectome. Nat Neurosci. 2016; 19:1100–1114. DOI: 10.1038/nn.4332 [PubMed: 27322419]

Honey CJ, Sporn O, Cammoun L, Gigandet X, Thiran JP, Meuli R, Hagmann P. Predicting human resting-state functional connectivity from structural connectivity. Proc Natl Acad Sci USA. 2009; 106(6):2035–2040. DOI: 10.1073/pnas.0811168106 [PubMed: 19188601]

Hoover JE, Hoffer ZS, Alloway KD. Projections from primary somatosensory cortex to the neostriatum: the role of somatotopic continuity in corticostriatal convergence. J Neurophysiol. 2003; 89:1576–1687. DOI: 10.1152/jn.01009.2002 [PubMed: 12611938]

Hoover WB, Vertes RP. Anatomical analysis of afferent projections to the medial prefrontal cortex in the rat. Brain Struct Funct. 2007; 212(2):149–179. DOI: 10.1007/s00429-007-0150-4 [PubMed: 17717690]

Hudetz AG. General anesthesia and human brain connectivity. Brain Connect. 2012; 2(6):291–302. DOI: 10.1089/brain.2012.0107 [PubMed: 23153273]

Hutchison RM, Leung LS, Mirsattari SM, Gati JS, Menon RS, Everling S. Resting-state networks in the macaque at 7T. NeuroImage. 2011; 56(3):1546–1555. DOI: 10.1016/j.neuroimage.2011.02.063 [PubMed: 21356313]

Hwang E, Kim S, Han K, Choi JH. Characterization of phase transition in the thalamocortical system during anesthesia-induced loss of consciousness. PLoS One. 2012; 7(12):e50580.doi: 10.1371/journal.pone.0050580 [PubMed: 23236379]

Jankowski MM, O'Mara SM. Dynamics of place, boundary and object encoding in rat anterior claustrum. Front Behav Neurosci. 2015; 9:250.doi: 10.3389/fnbeh.2015.00250 [PubMed: 26557060]

Author Manuscript Author Manuscript Author Manuscript Author Manuscript

Joksovic PM, Todorovic SM. Isoflurane modulates neuronal excitability of the nucleus reticularis thalami in vitro. Ann NY Acad Sci. 2010; 1199:36–42. DOI: 10.1111/j.1749-6632.2009.05172.x [PubMed: 20633107]

Koubeissi MZ, Bartolomei F, Beltagy A, Picard F. Electrical stimulation of a small brain area reversibly disrupts consciousness. Epilepsy Behav. 2014; 37:32–35. DOI: 10.1016/j.yebeh.2014.05.027 [PubMed: 24967698]

Künzle H. Bilateral projections from precentral motor cortex to the putamen and other parts of the basal ganglia: an autoradiographic study in Macaca fascicularis. Brain Res. 1975; 88(2):195–209. [PubMed: 50112]

Langmoen IA, Larsen M, Berg-Johnsen J. Volatile anaesthetics: cellular mechanisms of action. Eur J Anaesthesiol. 1995; 12:51–58. [PubMed: 7535694]

LeVay S, Sherk H. The visual claustrum of the cat. II. The visual field map. J Neurosci. 1981; 1(9):981–992. [PubMed: 6169811]

Liachenko S, Tang P, Somogyi GT, Xu Y. Concentration dependent isoflurane effects on depolarization-evoked glutamate and GABA outflows from mouse brain slices. Br J Pharmacol. 1999; 127:131–138. DOI: 10.1038/sj.bjp.0702543 [PubMed: 10369465]

Liang Z, Jean K, Zhang N. Uncovering intrinsic connectional architecture of functional networks in awake rat brain. J Neurosci. 2011; 31(10):3776–3783. DOI: 10.1523/JNEUROSCI.4557-10.2011 [PubMed: 21389232]

Liang Z, Jean K, Zhang N. Intrinsic organization of the anesthetized brain. J Neurosci. 2012; 32(30):10183–10191. DOI: 10.1523/JNEUROSCI.1020-12.2012 [PubMed: 22836253]

Liang Z, Liu X, Zhang N. Dynamic resting state functional connectivity in awake and anesthetized rodents. Neuroimage. 2015; 104:89–99. DOI: 10.1016/j.neuroimage.2014.10.013 [PubMed: 25315787]

Liu X, Pillay S, Li Rupeng, Vizuete JA, Pechman KR, Schmainda KM, Hudetz AG. Multiphasic modification of intrinsic functional connectivity of the rat brain during increasing levels of propofol. Neuroimage. 2013; 83:581–592. DOI: 10.1016/j.neuroimage.2013.07.003 [PubMed: 23851326]

Liu X, Zhu XH, Zhang Y, Chen W. Neural origin of spontaneous hemodynamic fluctuations in rats under burst-suppression anesthesia condition. Cerebral Cortex. 2011; 21(2):374–384. DOI: 10.1093/cercor/bhq105 [PubMed: 20530220]

Lu H, Zou Q, Gu H, Raichle ME, Stein EA, Yang Y. Rat brains also have a default mode network. Proc Natl Acad Sci USA. 2012; 109(10):3979–3984. DOI: 10.1073/pnas.1200506109 [PubMed: 22355129]

Masamoto K, Kanno I. Anesthesia and the quantitative evaluation of neurovascular coupling. J Cereb Blood Flow Metab. 2012; 32:1233–1247. DOI: 10.1038/jcbfm.2012.50 [PubMed: 22510601]

Mashour GA. Integrating the science of consciousness and anesthesia. Anesth Analg. 2006; 103(4):975–982. DOI: 10.1213/01.ane.0000232442.69757.4a [PubMed: 17000815]

Mathur BN, Caprioli RM, Deutch AY. Proteomic analysis illuminates a novel structural definition of the claustrum and insula. Cereb Cortex. 2009; 19(10):2372–2379. DOI: 10.1093/cercor/bhn253 [PubMed: 19168664]

Mathur BN. The claustrum in review. Front Syst Neurosci. 2014; 8:48.doi: 10.3389/fnsys.2014.00048 [PubMed: 24772070]

Milardi D, Bramanti P, Milazzo C, Finocchio G, Arrigo A, Santoro G, Trimarchi F, Quararone A, Anastasi G, Gaeta M. Cortical and subcortical connections of the human claustrum revealed in vivo by constrained spherical deconvolution tractography. Cereb Cortex. 2013; 25(2):406–414. DOI: 10.1093/cercor/bht231 [PubMed: 24014669]

Mitchell AS. The mediodorsal thalamus as a higher order thalamic relay nucleus important for learning and decision-making. Neurosci Biobehav Rev. 2015; 54:76–88. DOI: 10.1016/j.neubiorev.2015.03.001 [PubMed: 25757689]

Mhuircheartaigh RN, Rosenorn-Lanng D, Wise R, Jbabdi S, Rogers R, Tracey I. Cortical and subcortical connectivity changes during decreasing levels of consciousness in humans: a functional magnetic resonance imaging study using propofol. J Neurosci. 2010; 30(27):9095–9102. DOI: 10.1523/JNEUROSCI.5516-09.2010 [PubMed: 20610743]

Author Manuscript Author Manuscript Author Manuscript Author Manuscript

Nasrallah FA, Tay HC, Chuang KH. Detection of functional connectivity in the resting mouse brain. NeuroImage. 2014; 86:417–424. DOI: 10.1016/j.neuroimage.2013.10.025 [PubMed: 24157920]

Negyessy L, Hamori J, Bentivoglio M. Contralateral cortical projection to mediodorsal thalamic nucleus: origin and synaptic organization in the rat. Neuroscience. 1998; 84(3):741–753. [PubMed: 9579780]

Olson CR, Graybiel AM. Sensory maps in the claustrum of the cat. Nature. 1980; 288:479–481. [PubMed: 7442793]

Park S, Tsyzka JM, Allman JM. The claustrum and insula in Microcebus murinus: a high resolution diffusion imaging study. Front Neuroanat. 2012; 6:21.doi: 10.3389/fnana.2012.00021 [PubMed: 22707933]

Paxinos, G., Watson, C. The rat brain in stereotaxic coordinates. 6th. Elsevier Academic Press; New York: 2006.

Peltier SJ, Kerssens C, Hamann SB, Sebel PS, Byas-Smith M, Hu X. Functional connectivity changes with concentration of sevoflurane anesthesia. Neuroreport. 2005; 16(3):285–288. [PubMed: 15706237]

Reep RL, Corwin JV. Posterior parietal cortex as part of a neural network for directed attention in rats. Neurobiol Learn Mem. 2009; 91(2):104–113. DOI: 10.1016/j.nlm.2008.08.010 [PubMed: 18824116]

Remedios R, Logothetis NK, Kayser C. Unimodal responses prevail within the multisensory claustrum. J Neurosci. 2010; 30(30):19902–12907. DOI: 10.1523/JNEUROSCI.2937-10.2010

Reser DH, Majka P, Snell S, Chan J, Watkins K, Worthy K, Quiroga DM, Rosa MGP. Topography of claustrum and insula projections to medial prefrontal and anterior cingulate cortex of the common marmoset (Callithrix jacchus). J Comp Neurol. 2016; doi: 10.1002/cne.24009

Ries CR, Puil E. Mechanism of anesthesia revealed by shunting actions of isoflurane on thalamocortical neurons. J Neurophysiol. 1999a; 81:1795–1801. [PubMed: 10200213]

Ries CR, Puil E. Ionic mechanism of isoflurane's action on thalamocortical neurons. J Neurophysiol. 1999b; 81:1802–1809. [PubMed: 10200214]

Schwarz A, Gass N, Sarorius A, Zheng L, Spedding M, Schenker E, Meyer-Lindberg A, Weber-Fahr W. Anti-correlated cortical networks of intrinsic connectivity in the rat brain. Brain Connect. 2013; 3:503–511. DOI: 10.1089/brain.2013.0168 [PubMed: 23919836]

Schroter MS, Spoormaker VI, Schorer A, Wohlschlager A, Czisch M, Kochs EF, Zimmer C, Hemmer B, Schneider G, Jordan D, Ilg R. Spatiotemporal Reconfiguration of Large-Scale Brain Functional Networks during Propofol-Induced Loss of Consciousness. J Neurosci. 2012; 32(37):12832–12840. DOI: 10.1523/JNEUROSCI.6046-11.2012 [PubMed: 22973006]

Seeley WW, Menon V, Schatzberg AF, Keller J, Glover GGH, Kenna H, Reiss AL, Greicius MD. Dissociable intrinsic connectivity networks for salience processing and executive control. J Neurosci. 2007; 27:2349–2356. DOI: 10.1523/JNEUROSCI.5587-06.2007 [PubMed: 17329432]

Sforazzini F, Bertero A, Dodero L, David G, Galbusera A, Scattoni M, Pasqualetti M, Gozzi A. Altered functional connectivity networks in acallosal and socially impaired BTBR mice. Brain Struct Func. 2014a; :1–14. DOI: 10.1007/s00429-014-0948-9

Sforazzini F, Schwarz AJ, Galbusera A, Bifone A, Gozzi A. Distributed BOLD and CBV-weighted resting-state networks in the mouse brain. Neuroimage. 2014b; 87:403–415. DOI: 10.1016/j.neuroimage.2013.09.050 [PubMed: 24080504]

Sherk, H. The claustrum and the cerebral cortex. Jones, EG., Peters, A., editors. Plenum; New York: 1986. p. 467-499.

Sherk, H. Physiology of the claustrum. In: Smythies, JR.Edelstein, LR., Ramachandran, VS., editors. The claustrum: structural, functional, and clinical neuroscience. Academic Press, Elsevier Inc.; San Diego: 2014. p. 177-191.

Sherman SM, Guillery RW. On the actions that one nerve cell can have on another: distinguishing "drivers" from "modulators". Proc Natl Acad Sci USA. 1998; 95:7121–7126. [PubMed: 9618549]

Shima K, Hoshi E, Tanji J. Neuronal activity of the claustrum of the monkey during performance of multiple movements. J Neurophysiol. 1991; 76(3):2115–2119.

Author Manuscript Author Manuscript Author Manuscript Author Manuscript

Shirey MJ, Smith JB, Kudlik DE, Huo BX, Greene SE, Drew PJ. Brief anesthesia, but not voluntary locomotion, significantly alters cortical temperature. J Neurophysiol. 2015; 114(1):309–322. DOI: 10.1152/jn.00046.2015 [PubMed: 25972579]

Smith JB, Alloway KD. Functional specificity of claustrum connections in the rat: interhemispheric communication between specific parts of motor cortex. J Neurosci. 2010; 30(50):16832–16844. DOI: 10.1523/JNEUROSCI.4438-10.2010 [PubMed: 21159954]

Smith JB, Mowery TM, Alloway KD. Thalamic POm projections to the dorsolateral striatum of rats: potential pathway for mediating stimulus-response associations for sensorimotor habits. J Neurophysiol. 2012a; 108:160–174. DOI: 10.1152/jn.00142.2012 [PubMed: 22496533]

Smith JB, Radhakrishnan H, Alloway KD. Rat claustrum coordinates but does not integrate somatosensory and motor cortical information. J Neurosci. 2012b; 32(25):8583–888. DOI: 10.1523/JNEUROSCI.1524-12.2012 [PubMed: 22723699]

Smith JB, Alloway KD. Interhemispheric claustral circuits coordinate sensory and motor cortical areas that regulate exploratory behaviors. Front Syst Neurosci. 2014; 8:93.doi: 10.3389/fnsys.2014.00093 [PubMed: 24904315]

Smythies J, Edelstein L, Ramachandran VS. Hypotheses relating to the function of the claustrum. Front Integr Neurosci. 2012; 6:53.doi: 10.3389/fnint.2012.00053 [PubMed: 22876222]

Smythies, J., Edelstein, L., Ramachandran, VS. The claustrum: structural, functional, and clinical neuroscience. Academic Press, Elsevier Inc.; San Diego: 2014.

Spector I, Hassmannova J, Albe-Fessard D. Sensory properties of single neurons of cat's claustrum. Brain Res. 1974; 66:39–65.

Taqliazucchi E, Chialvo DR, Siniatchkin M, Amico E, Brichant JF, Bonhomme V, Noirhomme Q, Laufs H, Laurey S. Large-scale signatures of unconsciousness are consistent with a departure from critical dynamics. J R Soc Interface. 2016; 13(114)doi: 10.1098/rsif.2015.1027

Vanhaudenhuyse A, Noirhomme Q, Tshibanda LJ, Bruno MA, Boveroux P, Schnakers C, Soddu A, Perlbarg V, Ledoux D, Brichant JF, Moonen G, Maquet P, Greicius MD, Laureys S, Boly M. Default network connectivity reflects the level of consciousness in non-communicative brain-damaged patients. Brain. 2010; 133:161–171. DOI: 10.1093/brain/awp313 [PubMed: 20034928]

Vertes RP. Differential projections of the infralimbic and prelimbic cortex in the rat. Synapse. 2004; 51(1):32–58. DOI: 10.1002/syn.10279 [PubMed: 14579424]

Vincent JL, Patel GH, Fox MD, Snyder AZ, Baker JT, Van Essen DC, Zempel JM, Snyder LH, Corbetta M, Raichle ME. Intrinsic functional architecture in the anaesthetized monkey brain. Nature. 2007; 447(7140):83–86. http://doi.org/10.1038/nature05758. [PubMed: 17476267]

Wakamori M, Ikemoto Y, Akaike N. Effects of two volatile anesthetics and a volatile convulsant on the excitatory and inhibitory amino acid responses in dissociated CNS neurons of the rat. J Neurophysiol. 1991; 66:2014–2021. [PubMed: 1667416]

Wang Q, Ng L, Harris JA, Feng D, Li Y, Royall JJ, Oh SW, Bernard A, Sunkin SM, Koch C, Zeng H. Organization of the connections between claustrum and cortex in the mouse. J Comp Neurol. 2016; doi: 10.1002/cne.24047

Ying SW, Werner DF, Homanics GE, Harrison NL, Goldstein PA. Isoflurane modulates excitability in the mouse thalamus via GABA- dependent and GABA-independent mechanisms. Neuropharmacology. 2009; 56(2):438–447. DOI: 10.1016/j.neuropharm.2008.09.015 [PubMed: 18948126]

Zingg B, Hinitryan H, Gou L, Song MY, Bay M, Bienkowski MS, Foster NN, Yamashita S, Bowman I, Toga AW, Dong HW. Neural networks of the mouse neocortex. Cell. 2014; 156(5):1096–1111. DOI: 10.1016/j.cell.2014.02.023 [PubMed: 24581503]

Author Manuscript Author Manuscript Author Manuscript Author Manuscript

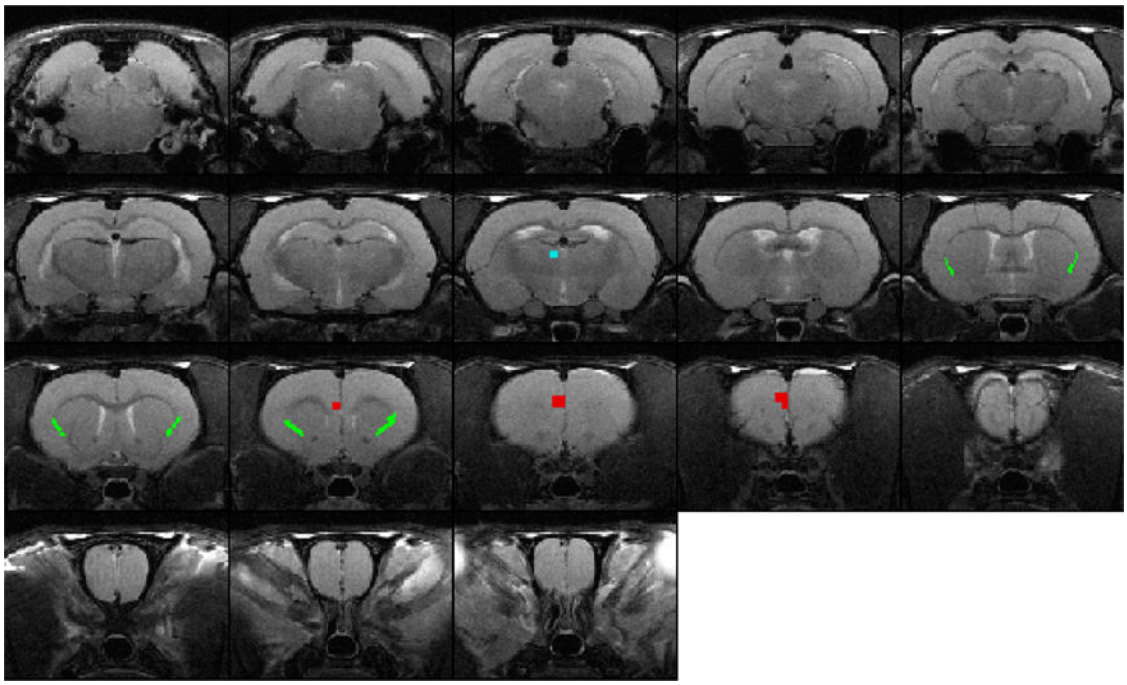

Fig. 1.

Location of claustrum seeds in structural MRI images. T1 weighted structural MRI images from a representative animal used as a template to align all animals. Colored pixels identify location of seed regions in claustrum (green), mPFC (red), and MD-thalamus (blue).

Author Manuscript Author Manuscript Author Manuscript Author Manuscript

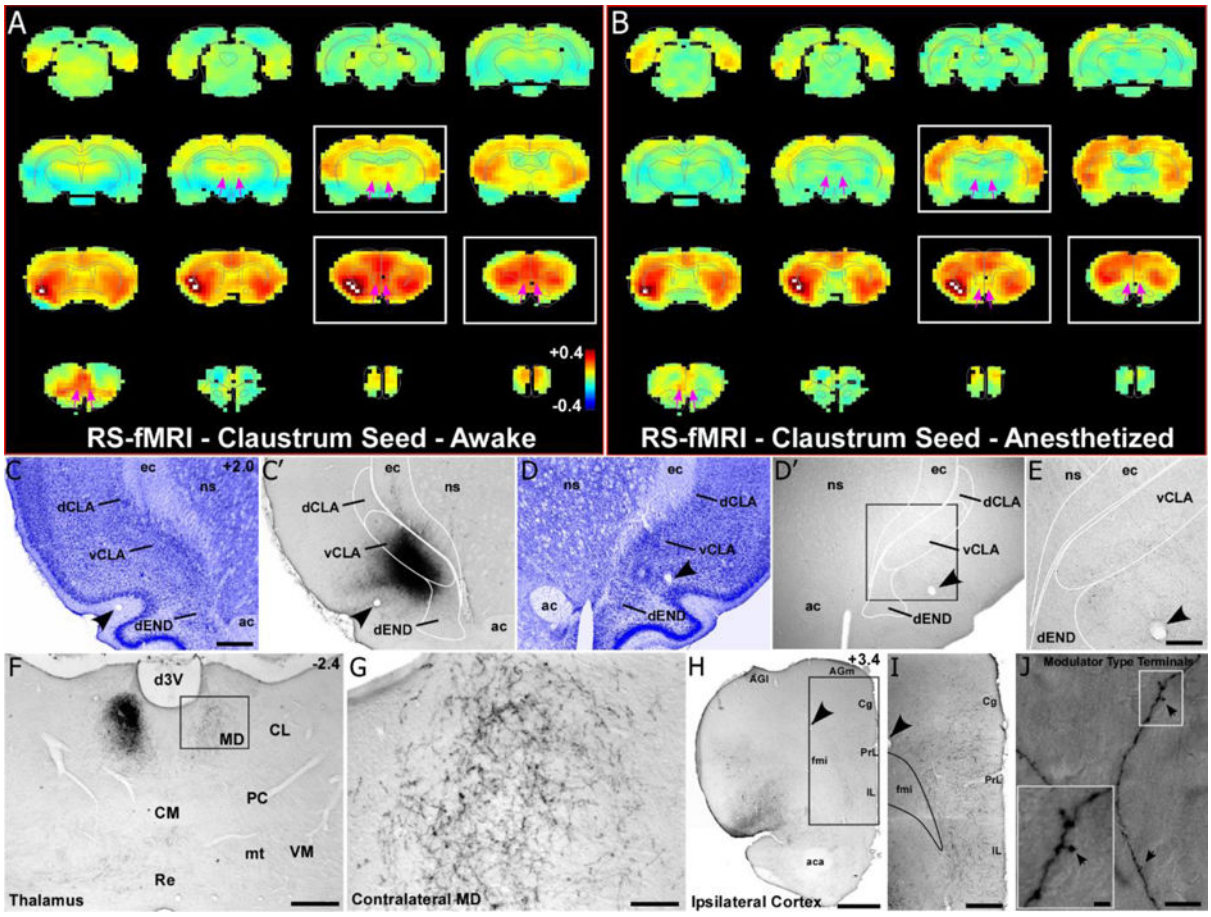

Fig. 2.

RS-fMRI in the awake state reveals bilateral functional connections of the claustrum that are lost during anesthesia. **(a)** Average RS-fMRI of awake rats, showing a unilateral seed (white voxels) based analysis of the claustrum. Strong functional connectivity was observed bilaterally between the claustrum, mediodorsal thalamus (MD), medial prefrontal cortex (mPFC), and several other cortical areas (including retrosplenial, sensorimotor and multimodal regions). The claustrum also displayed functional connectivity with the contralateral claustrum. White boxes correspond to sections shown in tracing data. Color bar represents correlation coefficients and applies to panel **b** as well. (**b)** Unilateral seed analysis of claustrum in anesthetized condition revealed abolished functional connectivity with MD and reduced functional connectivity with mPFC (see pink arrows). (**c)** Nissl stained section showing cytoarchitecture of the dorsal and ventral claustrum (dCLA, vCLA) and dorsal endopiriform nucleus (dEND) with adjacent section (**c′**) showing an anterograde tracer injection (BDA) primarily in vCLA (abbreviations: ec, external capsule; ns, neostriatum; ac, anterior commissure). Scale bar in **c**, 500μm. (**c–e)** Labeling is absent in the contralateral claustrum despite a strong functional connection detected by RS-fMRI in panels **a** and **b**. Scale bar in **e**, 250μm. (**f–g)** Bilateral labeling in MD, which matches bilateral functional connectivity. Scale bars: 500μm in **f**; 100μm in **g**. (**h–i)** Terminal labeling in ipsilateral mPFC, distributed across all layers of cortex (abbreviations: AGl, agranular lateral; AGm, agranular medial; Cg, cingulate; PrL, prelimbic; IL, infralimbic; fmi, forceps minor of the

corpus callosum; aca, anterior commissure). Scale bars: 1mm in **h**; 500μm in **i**) **(j)** Claustro-cortical synaptic terminals have modulator-type morphology (black arrows). Scale bars: 10μm in (**j)**; 2μm in inset.

Author Manuscript Author Manuscript Author Manuscript Author Manuscript

Author Manuscript Author Manuscript Author Manuscript Author Manuscript

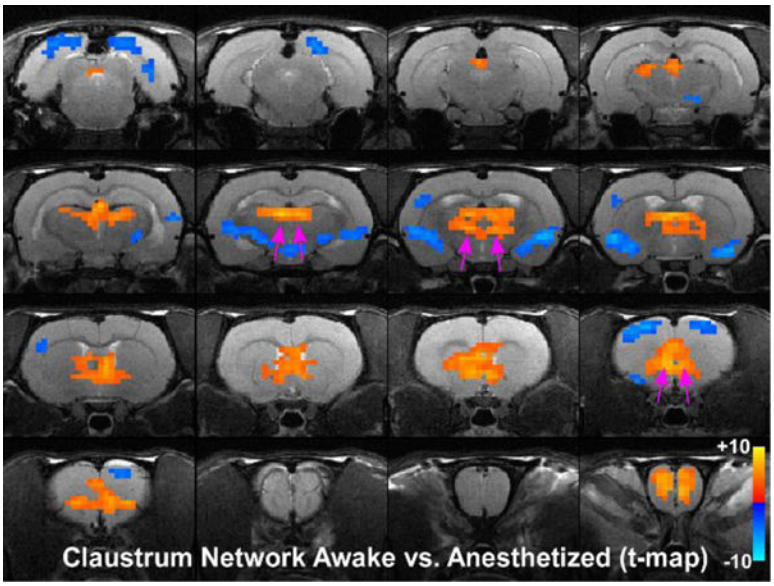

Fig. 3.

Statistical analysis comparing claustrum seed in the awake and anesthetized states. Colored pixels represent significant t-values (two-tailed t-tests) with $p<0.05$ based on False Discovery Rate that are overlain on the T1 weighted structural MRI template. Positive t-values indicate pixels where functional connections were stronger in the awake state compared to the deeply anesthetized state. Pink arrows point to significant positive t-values for MD-thalamus and mPFC.

Author Manuscript Author Manuscript Author Manuscript Author Manuscript

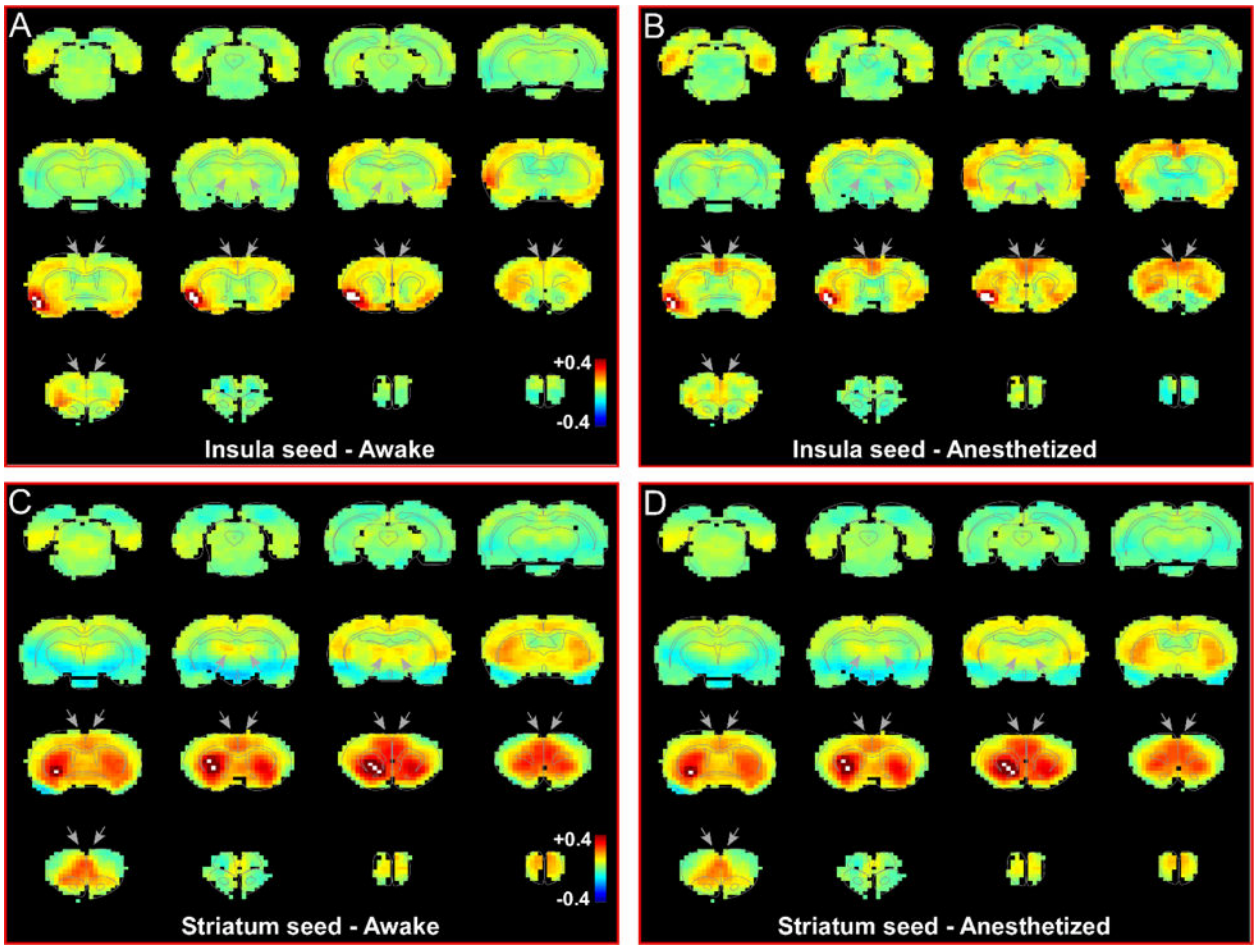

Fig. 4.

Resting state functional network of insular cortex and striatum are different from the claustrum. **(a)** RS-fMRI analysis with unilateral seed in insular cortex during awake state. Grey arrows indicate regions of high correlation with the claustrum that show no correlation with insula. **(b)** RS-fMRI analysis with unilateral seed in insular cortex during anesthetized state. **(c)** RS-fMRI analysis with unilateral seed in striatum during awake state. Grey arrows indicate regions of high correlation with the claustrum. **(d)** RS-fMRI analysis with unilateral seed in striatum during anesthetized state. White pixels represent seed region. Color bar represents correlation coefficients.

Author Manuscript Author Manuscript Author Manuscript Author Manuscript

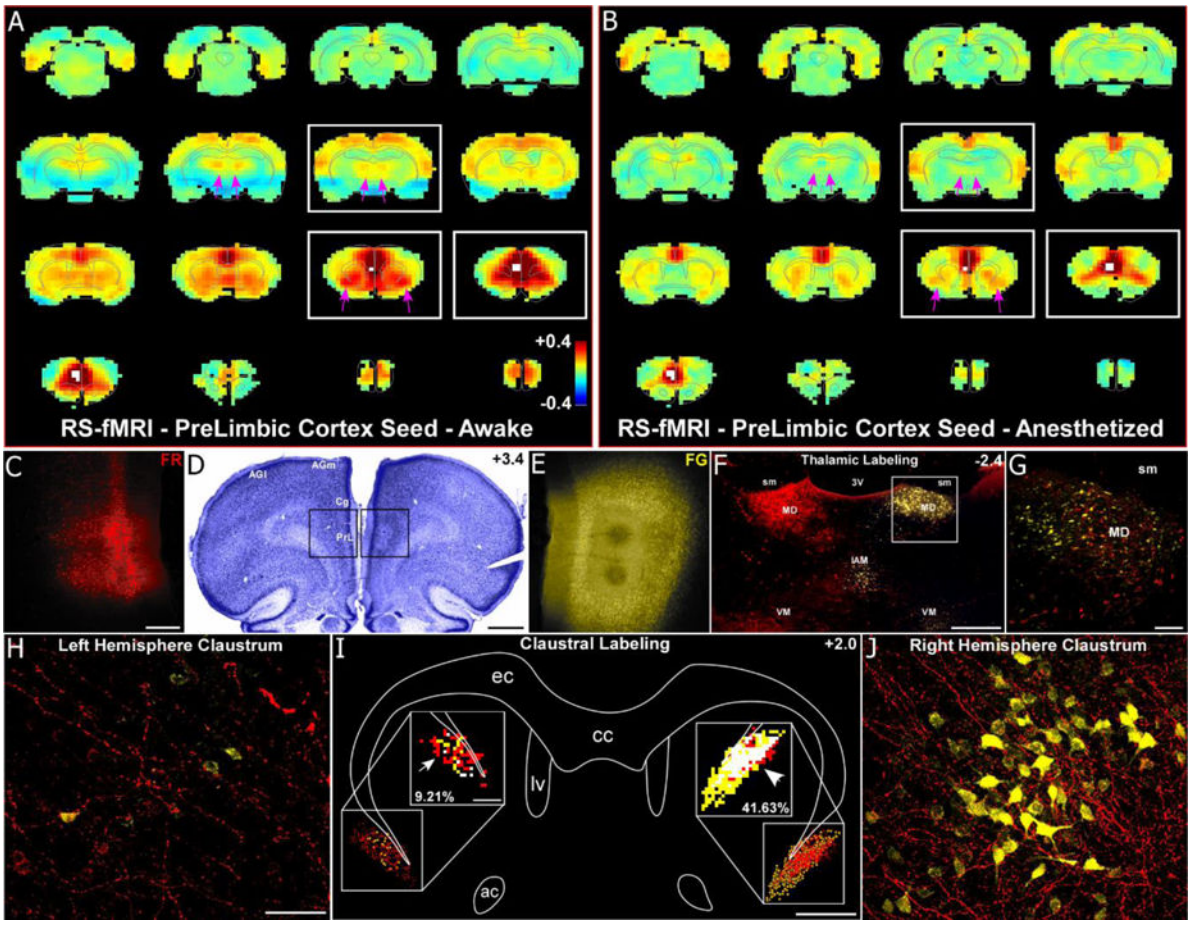

Fig. 5.

RS-fMRI in the awake state reveals functional connections of the mPFC that are lost during anesthesia. **(a)** Average RS-fMRI of awake rats, with a unilateral seed (white voxels) in mPFC (prelimbic cortex, PrL). Bilateral functional connectivity was observed between mPFC and the claustrum, mediodorsal thalamus (MD), and retrosplenial and entorhinal cortices. Color bar represents correlation coefficients and applies to panel **b** as well. (**b)** Anesthesia abolished functional connectivity with MD and severely reduced functional connectivity with claustrum (see pink arrows). (**c–e)** Anterograde tracer (Fluororuby, FR, red, left hemisphere, panel **c**) and retrograde tracer (Fluorogold, FG, yellow, right hemisphere, panel **e**) injections in PrL revealed anatomical connectivity with MD and claustrum. Scale bars: 250μm in **c**; 1mm in **d**. (**f–g)** Labeling was predominantly ipsilateral in the thalamus for both tracers. Anterogradely-labeled terminals were also observed in contralateral MD, terminating around retrogradely-labeled neurons, demonstrating an interhemispheric cortico-thalamo-cortical loop. Scale bars: 500μm in **f**; 100μm in **g**. Abbreviations: sm, stria medularis; 3V, third ventricle, interanteromedial nucleus, IAM; ventromedial nucleus, VM. (**h–j)** Anterograde projections terminated in the contralateral claustrum, intermingling with retrogradely-labeled FG neurons (panel **j**), demonstrating an interhemispheric cortico-claustro-cortical loop. Panel **i** shows a digital reconstruction of tracer labeling in claustrum and overlap analysis (50μm^2 bins) in the insets. Overlapping bins (white) contained at least 4 FR-labeled terminals and 1 FG-labeled neuron. Scale bars:

50μm in **h**; 1mm in **i**, 200μm in inset of **i**. Abbreviations: cc, corpus callosum; ec, external capsule; lv, lateral ventricle; ac, anterior commissure.

Author Manuscript Author Manuscript Author Manuscript Author Manuscript

Author Manuscript Author Manuscript Author Manuscript Author Manuscript

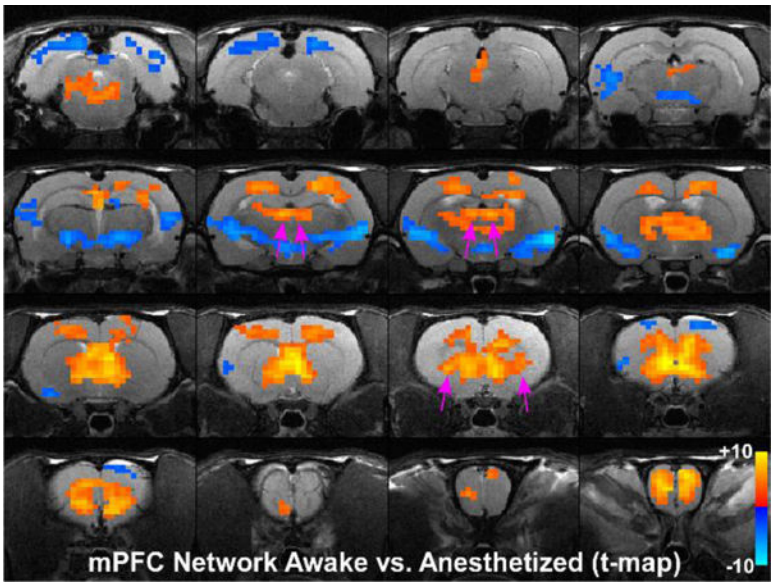

Fig. 6.

Statistical analysis comparing mPFC seed in the awake and anesthetized states. Colored pixels represent significant t-values (two-tailed t-tests) with $p<0.05$ based on False Discovery Rate that are overlain on the T1 weighted structural MRI template. Positive t-values indicate pixels where functional connections were stronger in the awake state compared to the deeply anesthetized state. Pink arrows point to significant positive t-values for MD-thalamus and claustrum.

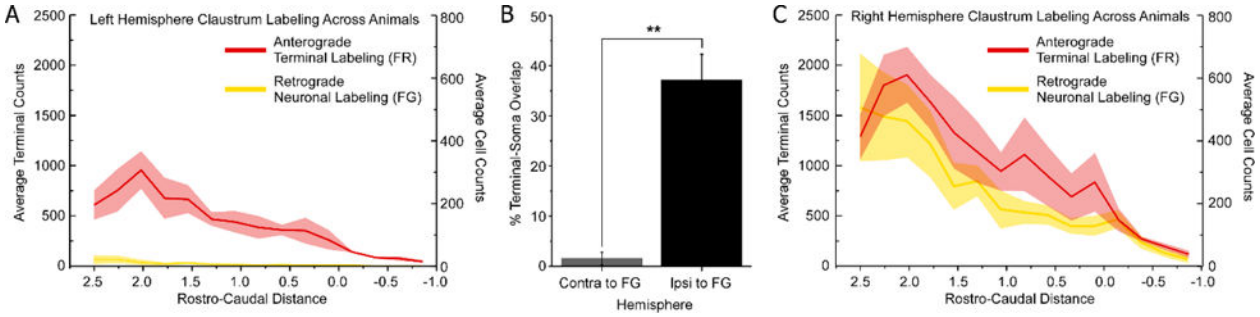

Fig. 7.

Quantification of tracer labeling from mPFC injections. (**a,c)** Average tracer labeling throughout the rostro-caudal extant of claustrum for all animals following anterograde and retrograde tracer injections into the left and right hemispheres, respectively. Solid lines represent means, shaded regions denote standard error of the mean (SEM). (**b)** Average percent overlap was much stronger in the hemisphere ipsilateral to the FG injection (**p<0.01). Error bars show SEM.

Author Manuscript Author Manuscript Author Manuscript Author Manuscript

Author Manuscript Author Manuscript Author Manuscript Author Manuscript

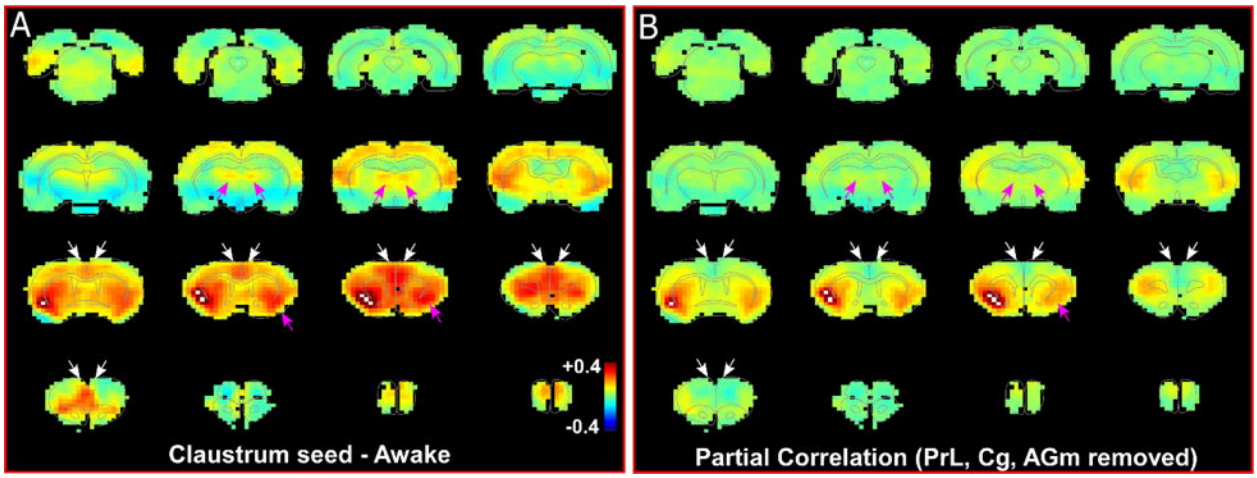

Fig. 8.

Partial correlation analysis shows loss of functional connectivity with contralateral claustrum after removal of mPFC correlations. **(a)** RS-fMRI analysis with unilateral seed in claustrum in right hemisphere during awake state. White arrows indicate regions of mPFC with removed correlations. Pink arrows identify MD and contralateral claustrum. White pixels represent seed region. Color bar represents correlation coefficients and applies to panel **b** as well. (**b)** RS-fMRI analysis showing partial correlation of unilateral claustrum seed after removal of correlations with prelimbic (PrL), cingulate (Cg) and agranular medial (AGm) cortical regions (mPFC).

Author Manuscript Author Manuscript Author Manuscript Author Manuscript

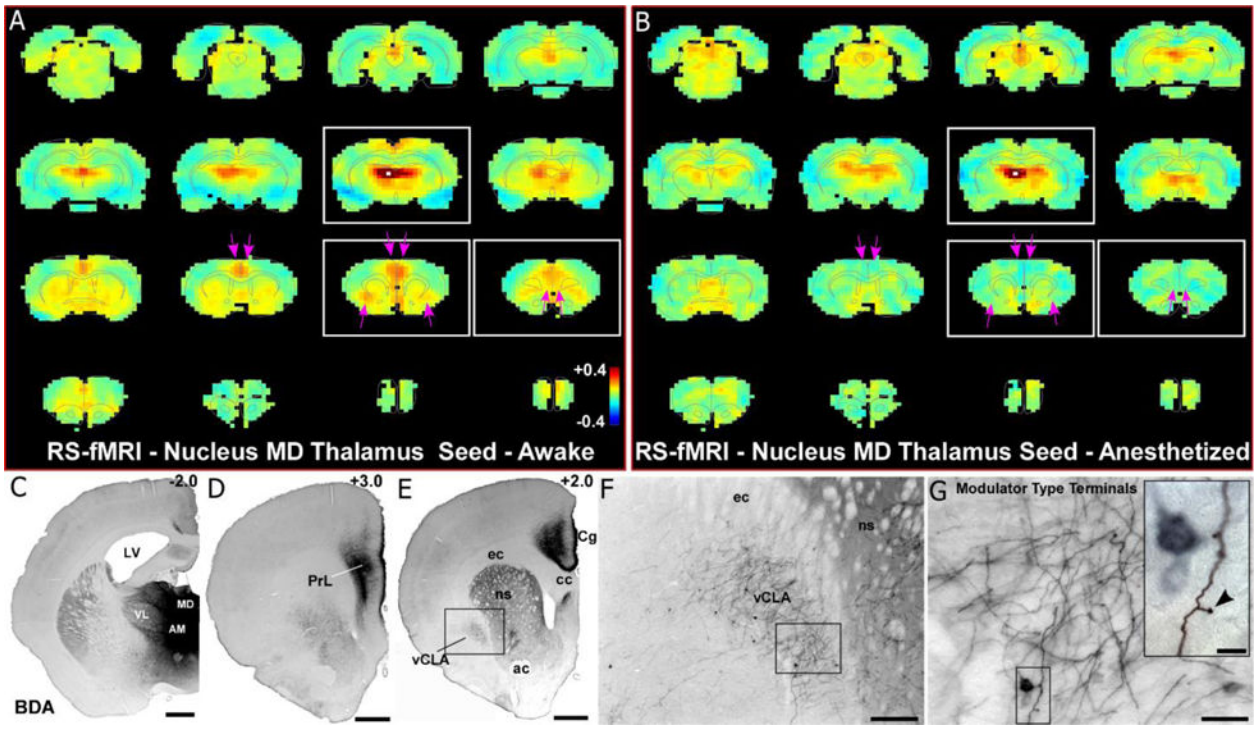

Fig. 9.

RS-fMRI analysis in the awake state reveals functional connections with the MD thalamus that are lost during anesthesia. **(a)** Average RS-fMRI of awake rats, with a unilateral seed (white voxels) in mediodorsal thalamus (MD). Strong functional connectivity was observed between MD and bilateral regions of mPFC and claustrum. Color bar represents correlation coefficients and applies to panel **b** as well. (**b)** Anesthesia abolished functional connectivity with both mPFC and claustrum (see pink arrows). (**c–e)** Anterograde tracer injection (panel **c**) into MD shows anatomical connectivity with mPFC (prelimbic cortex, PrL; cingulate cortex, Cg) shown in panels **d** and **e**, as well as claustrum (panel **e**). Scale bars: 1mm in **c**, **d**, **e**. Abbreviations: AM, anteromedial nucleus; VL, ventrolateral nucleus; LV, lateral ventricle; cc, corpus callosum; ec, external capsule; ns, neostriatum; ac, anterior commissure. (**f)** Higher magnification image of claustrum labeling from inset in **e**, showing both anterogradely-labeled fibers and retrogradely-labeled neurons. Scale bar: 250μm. (**g)** Higher magnification image of labeling from inset in **f**, showing projections from MD to claustrum are thin fibers with small modulator type terminals. Scale bars: 50μm in **g**; 10μm in inset.

Author Manuscript Author Manuscript Author Manuscript Author Manuscript

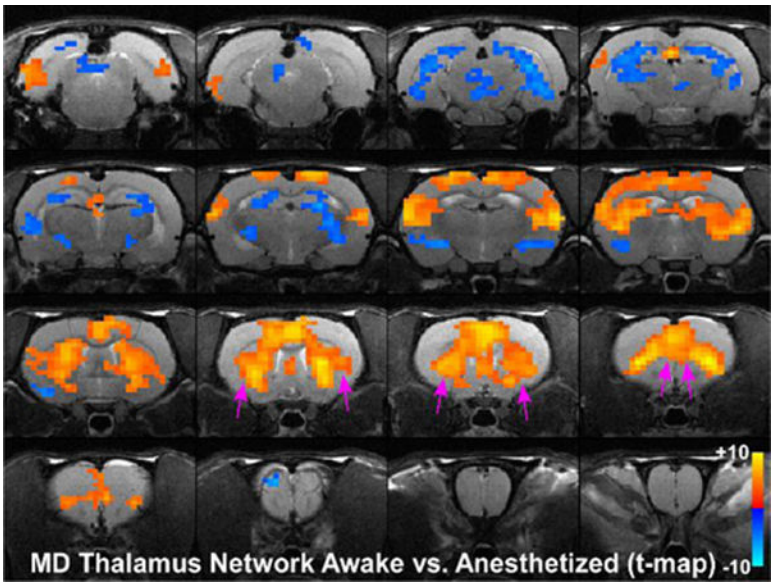

Fig. 10.

Statistical analysis comparing MD seed in the awake and anesthetized states. Colored pixels represent significant t-values (two-tailed t-tests) with $p<0.05$ based on False Discovery Rate that are overlain on the T1 weighted structural MRI template. Positive t-values indicate pixels where functional connections were stronger in the awake state compared to the deeply anesthetized state. Pink arrows point to significant positive t-values for claustrum and mPFC.

Author Manuscript Author Manuscript Author Manuscript Author Manuscript

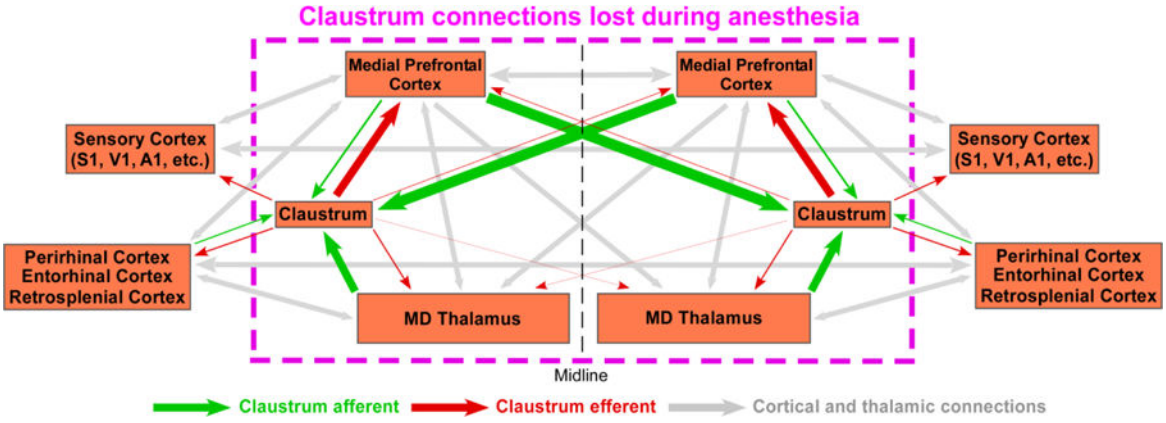

Fig. 11.

Circuit diagram of claustrum connectivity. Circuit diagram showing the connections of the claustrum based on the findings from this paper and cited references. Enclosed in the pink, dashed box are the brain regions shown by RS-fMRI to be lost in the transition from the awake to the anesthetized state. Line widths correspond to strength of anatomical connections.